Neuron

Article

Endocannabinoid Actions on Cortical Terminals Orchestrate Local Modulation of Dopamine Release in the Nucleus Accumbens

Highlights

- Cannabinoids and endocannabinoids inhibit dopamine release in nucleus accumbens
- This involves CB1 receptors on afferents from prefrontal cortex
- Cholinergic and glutamatergic synapses drive CB1-sensitive dopamine release
- CB1 receptors on prefronto-accumbens afferents modulate reward-driven behavior

Authors

Yolanda Mateo, Kari A. Johnson, Dan P. Covey, ..., Marisela Morales, Joseph F. Cheer, David M. Lovinger

Correspondence

jcheer@som.umaryland.edu (J.F.C.), lovindav@mail.nih.gov (D.M.L.)

In Brief

Mateo et al. demonstrate that glutamate and acetylcholine-driven dopamine release in the nucleus accumbens is modulated by CB1 receptors on prefrontal cortical afferents. Endogenous activation of these receptors modifies dopamine-dependent reward-driven behavior sustained by optical activation of prefrontal cortical terminals.

Mateo et al., 2017, Neuron *96*, 1112–1126
December 6, 2017 Published by Elsevier Inc.
https://doi.org/10.1016/j.neuron.2017.11.012

CellPress

Neuron
Article

Endocannabinoid Actions on Cortical Terminals Orchestrate Local Modulation of Dopamine Release in the Nucleus Accumbens

Yolanda Mateo,[1] Kari A. Johnson,[1] Dan P. Covey,[2] Brady K. Atwood,[1] Hui-Ling Wang,[3] Shiliang Zhang,[3] Iness Gildish,[2] Roger Cachope,[2] Luigi Bellocchio,[4] Manuel Guzmán,[4] Marisela Morales,[3] Joseph F. Cheer,[2,5,6,*] and David M. Lovinger[1,6,7,*]

[1]Section on Synaptic Pharmacology, Laboratory for Integrative Neuroscience, National Institute on Alcohol Abuse and Alcoholism, US National Institutes of Health, Rockville, MD, USA

[2]Department of Anatomy and Neurobiology, University of Maryland School of Medicine, Baltimore, MD, USA

[3]Neuronal Networks Section, National Institute on Drug Abuse, US National Institutes of Health, Baltimore, MD, USA

[4]Department of Biochemistry and Molecular Biology I, Centro de Investigacio´n Biomédica en Red sobre Enfermedades Neurodegenerativas (CIBERNED), Instituto Ramó n y Cajal de Investigación Sanitaria (IRYCIS) and Instituto Universitario de Investigacio´n Neuroquímica (IUIN), Complutense University, Madrid, Spain

[5]Department of Psychiatry, University of Maryland School of Medicine, Baltimore, MD, USA

[6]These authors contributed equally

[7]Lead Contact

*Correspondence: jcheer@som.umaryland.edu (J.F.C.), lovindav@mail.nih.gov (D.M.L.)

https://doi.org/10.1016/j.neuron.2017.11.012

SUMMARY

Dopamine (DA) transmission mediates numerous aspects of behavior. Although DA release is strongly linked to firing of DA neurons, recent developments indicate the importance of presynaptic modulation at striatal dopaminergic terminals. The endocannabinoid (eCB) system regulates DA release and is a canonical gatekeeper of goal-directed behavior. Here we report that extracellular DA increases induced by selective optogenetic activation of cholinergic neurons in the nucleus accumbens (NAc) are inhibited by CB1 agonists and eCBs. This modulation requires CB1 receptors on cortical glutamatergic afferents. Dopamine increases driven by optogenetic activation of prefrontal cortex (PFC) terminals in the NAc are similarly modulated by activation of these CB1 receptors. We further demonstrate that this same population of CB1 receptors modulates optical self-stimulation sustained by activation of PFC afferents in the NAc. These results establish local eCB actions on PFC terminals within the NAc that inhibit mesolimbic DA release and constrain reward-driven behavior.

INTRODUCTION

The role of dopamine (DA) in adaptive behaviors such as motivation, action control, and learning has been extensively studied. Regulation of DA release at axon terminals is governed by changes in firing rate of DA neurons. However, new evidence supporting the relevance of alterations in DA release from terminals in the striatum is emerging (Cachope and Cheer, 2014) with the interplay between glutamatergic and cholinergic systems drawing most attention (Cachope et al., 2012; Threlfell et al., 2012; Zhou et al., 2001). Endogenous cannabinoids (eCBs) are critical modulators of motivated behaviors, partly through their actions on rostral dopaminergic projections to the nucleus accumbens (NAc) (Oleson et al., 2012). However, dopaminergic neurons do not express cannabinoid type 1 (CB1) receptors (Julian et al., 2003). Therefore, the actions of eCBs and exogenous cannabinoids at the level of the dopaminergic cell bodies in the ventral tegmental area (VTA) are indirect and likely involve disinhibition of dopaminergic neurons via decreased GABA release at CB1-expressing inhibitory afferents (Cheer et al., 2000b; Lupica et al., 2004; Riegel and Lupica, 2004). This disinhibition likely produces enhanced phasic DA concentrations in the extracellular space within the NAc (Cheer et al., 2004; Oleson et al., 2012). On the other hand, it is not clear how CB1 receptors locally regulate DA release in terminal regions such as the NAc, due to the large number of convergent neural messengers involved. The NAc is crucial for the generation of motivated behaviors and integrates dopaminergic reinforcement signals with glutamate-encoded environmental stimuli to produce motor sequences that underlie goal-directed actions (Floresco, 2015). Importantly, medium spiny neurons (MSNs) of the NAc contain a molecular arrangement consistent with the on-demand production of eCBs and retrograde signaling via CB1 receptor activation (Uchigashima et al., 2007).

Prefrontal glutamatergic afferents to the NAc have long been theorized to carry information about exteroceptive triggers and contextual information (Sesack and Grace, 2010), and characterization of the behavioral effects of activating these afferents has been reported (Britt et al., 2012). However, there is virtually no information regarding the presynaptic modulation of glutamate release by CB1 receptor activation as it pertains to rapid DA dynamics within the NAc. Nevertheless, studies demonstrate that several forms of excitatory synaptic plasticity in the NAc

(Mato et al., 2005, 2008; Robbe et al., 2002a, 2002b), as well as in the dorsal striatum, require eCB signaling (Atwood et al., 2014; Gerdeman et al., 2002; Kreitzer and Malenka, 2005; Ronesi et al., 2004). These effects have predominantly involved CB1 receptor activation on glutamatergic terminals impinging upon MSNs and in some cases require D2 DA (Gerdeman et al., 2002) or metabotropic glutamate receptor 5 ($mGluR_5$) activation (Kreitzer and Malenka, 2005).

Another possible target for CB1 receptor modulation of phasic DA release within the NAc is the cholinergic interneuron (CIN) population, which exerts a profound influence on DA terminals, as its selective activation potently increases DA release independent of cell bodies in the VTA (Cachope et al., 2012; Threlfell et al., 2012). Indeed, endogenous acetylcholine (ACh) release promotes depolarization-induced mobilization of eCBs from MSNs (Narushima et al., 2007; Narushima et al., 2006). Additionally, NAc CINs co-release glutamate, and the cooperative action of DA and glutamate generates plastic changes in synaptic strength that underlie contrast enhancement of cues and action selection (Cachope et al., 2012; Higley et al., 2011).

To clarify how CB1 receptors within the NAc modulate DA release independently from cell bodies in the midbrain, we utilized a combination of electron microscopy, immunohistochemistry, pharmacology, electrophysiology, electrochemistry, and optogenetics. We also utilized cre-lox recombination to generate conditional knockout mouse models to test our hypotheses. We report that accumbal CB1 receptors are present in prefrontal terminals and that their specific genetic ablation eliminates CB1 receptor agonist-mediated inhibition of CIN-driven DA release. We further provide evidence that CIN activation recruits production of the eCB 2-arachidonoylglycerol (2-AG) to activate CB1 receptors on cortical glutamatergic terminals to modulate DA release. Critically, 2-AG mobilization influences behavior reinforced by optical activation of prefrontal cortical terminals in the NAc. These results uncover the intricate and precise nature of eCB signaling within different nodes of a common anatomical framework and provide another crucial target for the modulation of mesolimbic DA release in reinforcement.

RESULTS

CB1 Receptor Activation Modulates DA Release Elicited by Selective Activation of Cholinergic Interneurons

Previous studies have suggested that cholinergic transmission can be potently modulated by CB1 receptor activation (Tzavara et al., 2008) and our published work has shown that selective CIN excitation enhances DA release in the NAc both *in vivo* and *in vitro* (Cachope et al., 2012). Thus, CB1 receptor activation may alter ACh release and thus indirectly modify CIN-driven DA release. To examine this possibility, we monitored the effect of WIN 55,212-2 (WIN) a CB1 receptor agonist on NAc DA release triggered by selective optical stimulation of accumbal CINs (Figures 1A and 1B). First, we replicated our previous findings (Cachope et al., 2012) and determined that *in vivo* DA release is triggered by endogenous release of ACh (Figure 1A). Next, we found that WIN (1.5 mg/kg, i.p.) significantly decreases CIN-driven DA release *in vivo* (Figures 1B and 1C; $p < 0.05$). We then aimed to further study this phenomenon mechanistically in a brain slice preparation (Figure 1D). We observed that bath application of WIN (1 M) significantly decreased DA peak levels evoked by CIN activation by an average of 42% ± 3% relative to pretreatment levels ($p < 0.001$; $n = 7$; Figure 1E), recapitulating the *in vivo* findings. Pretreatment with the CB1 receptor antagonist AM251 (3 M) prevented WIN-elicited decreases in CIN-driven DA release ($n = 5$; Figures 1D–1F), confirming the involvement of CB1 receptors in this modulation.

CB1 Receptors Are Not Localized on Cholinergic Interneurons within the Nucleus Accumbens

The above-described data could be explained most parsimoniously by the presence of CB1 receptors on cholinergic terminals. Therefore, we used CB1 radioactive antisense riboprobes to examine the expression of CB1 mRNA in the NAc. We closely inspected individual ChAT immunoreactive neurons in the core and shell portions of the NAc to determine whether ChAT immunoreactivity co-localized with CB1 mRNA, but did not observe significant expression of CB1 mRNA in ChAT-expressing neurons in any of the NAc sub-fields studied (Figure S1A). This finding is none too surprising given previous data indicating no CB1 receptor expression in CINs within the NAc (Hohmann and Herkenham, 2000). As a complementary functional approach to determine if CB1 receptors on cholinergic terminals contribute to the inhibition of DA release, we generated conditional mutant mice in which CB1 was removed from cholinergic neurons by crossing $CB1^{flox/flox}$ mice with ChAT::cre mice. We confirmed that this approach was successful by measuring a significant decrease in CB1 mRNA in ChAT positive cells of ChAT cre_$CB1^{flox/flox}$ mice within the lateral septum (Figure S2). Next, we optically evoked CIN-driven DA release in the NAc and applied WIN (1 M) to the slice. Recordings from ChAT::cre/$CB1^{flox/flox}$ mice showed a WIN-induced depression of CIN-evoked DA release that was indistinguishable from that observed in ChAT::cre mice, consistent with a lack of CB1 receptor expression on CINs ($p < 0.0001$; $n = 5$; Figure S1B). Therefore, the regulation of DA release evoked by selective activation of CINs likely involves CB1 receptors at sites other than CINs themselves.

CB1 Receptor Modulation of Cholinergic Interneuron-Driven DA Release Requires Glutamatergic Transmission

Our prior work demonstrated that glutamate signaling at AMPA receptors contributes to CIN-evoked DA release (Cachope et al., 2012). As CIN-driven DA release is sensitive to CB1 receptor activation and CINs do not express CB1 receptors, we next tested whether the effect of WIN on CIN-evoked DA involves an indirect mechanism whereby CB1 receptors dampen glutamatergic drive to CINs. We first assessed whether optical activation of CINs elicited oEPSCs recorded from MSNs. Optical activation of CINs produced measureable oEPSCs (Figures 2A and 2B), as seen in previous work (Cachope et al., 2012; Higley et al., 2011; Threlfell et al., 2012). oEPSC amplitude remained stable throughout the length of the recordings (Figure 2B; 104% ± 4% baseline). Moreover, these oEPSCs appeared to have two components and a relatively long latency to peak, consistent with a disynaptic effect (Figure S3A). A 10-min bath

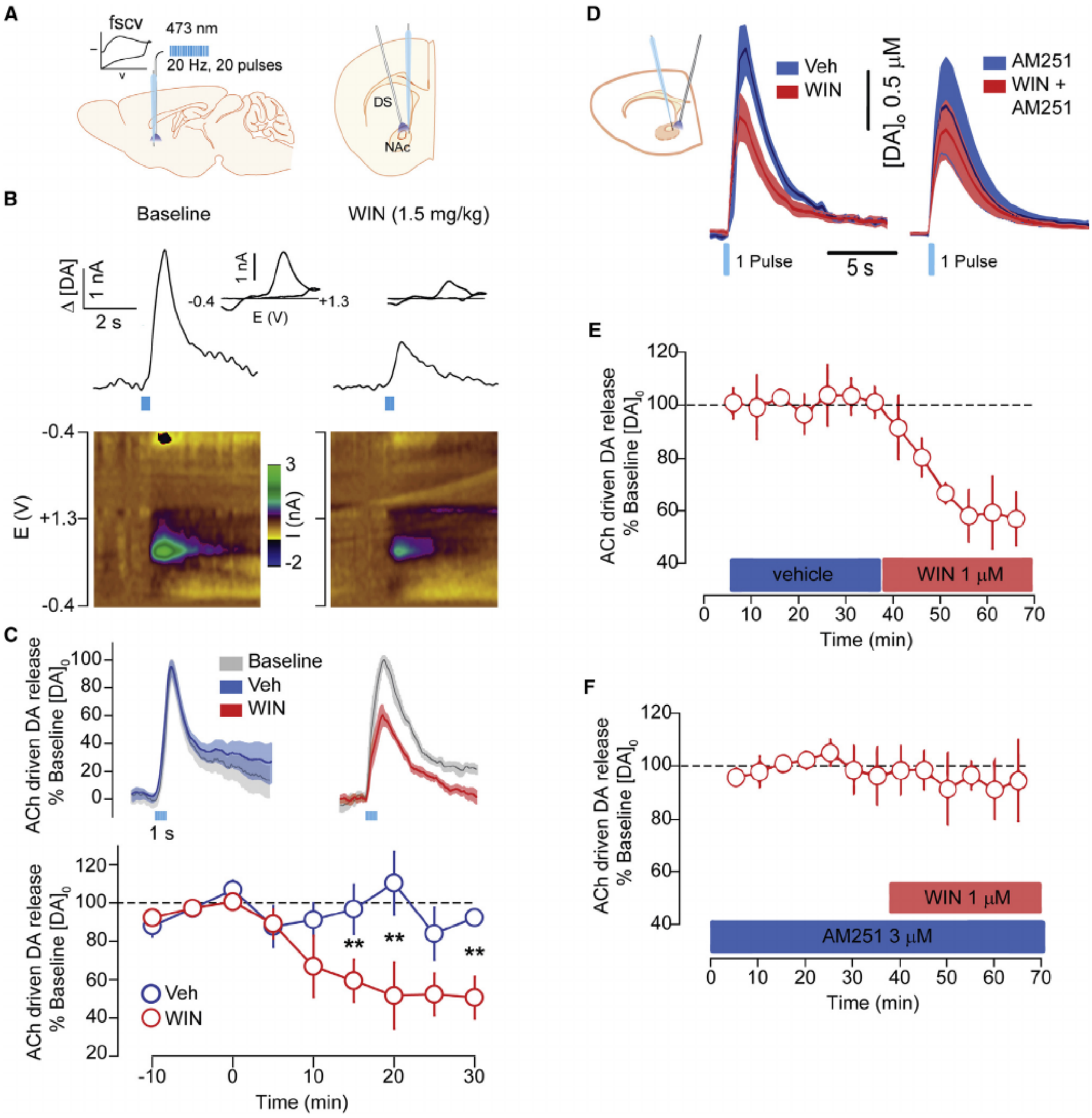

Figure 1. CB1 Receptor Activation Inhibits DA Release Driven by Selective Activation of Cholinergic Interneurons

(A) Anesthetized preparation for recording CIN-evoked DA release. Light stimulation (473 nm at 20 Hz) was delivered to NAc CINs through an optical fiber placed at 15 degrees relative to a carbon-fiber FSCV electrode.

(B) Representative *in vivo* recordings showing that the cannabinoid receptor agonist WIN55,212-2 (WIN) attenuates CIN-evoked DA release. DA was electrochemically identified based on ''cyclic voltammograms'' (inset) displaying changes in current (y axis) across the applied potential (x axis, E(V)) and pseudo-color plots (bottom panel) of serial cyclic voltammograms plotted across time (x axis), displaying changes in current (z axis) across the applied potential (y axis).

(C) Average (±SEM) CIN-evoked DA release recorded *in vivo* (top panel) at baseline and following vehicle (Veh, left panel; n = 5) and WIN (right panel; n = 5) treatment. Time course of peak CIN-driven $[DA]_O$ (bottom panel) prior to (10 to 0 min) and following VEH or WIN treatment (treatment time: $F_{(8,55)} = 2.45$, $p = 0.02$).

(legend continued on next page)

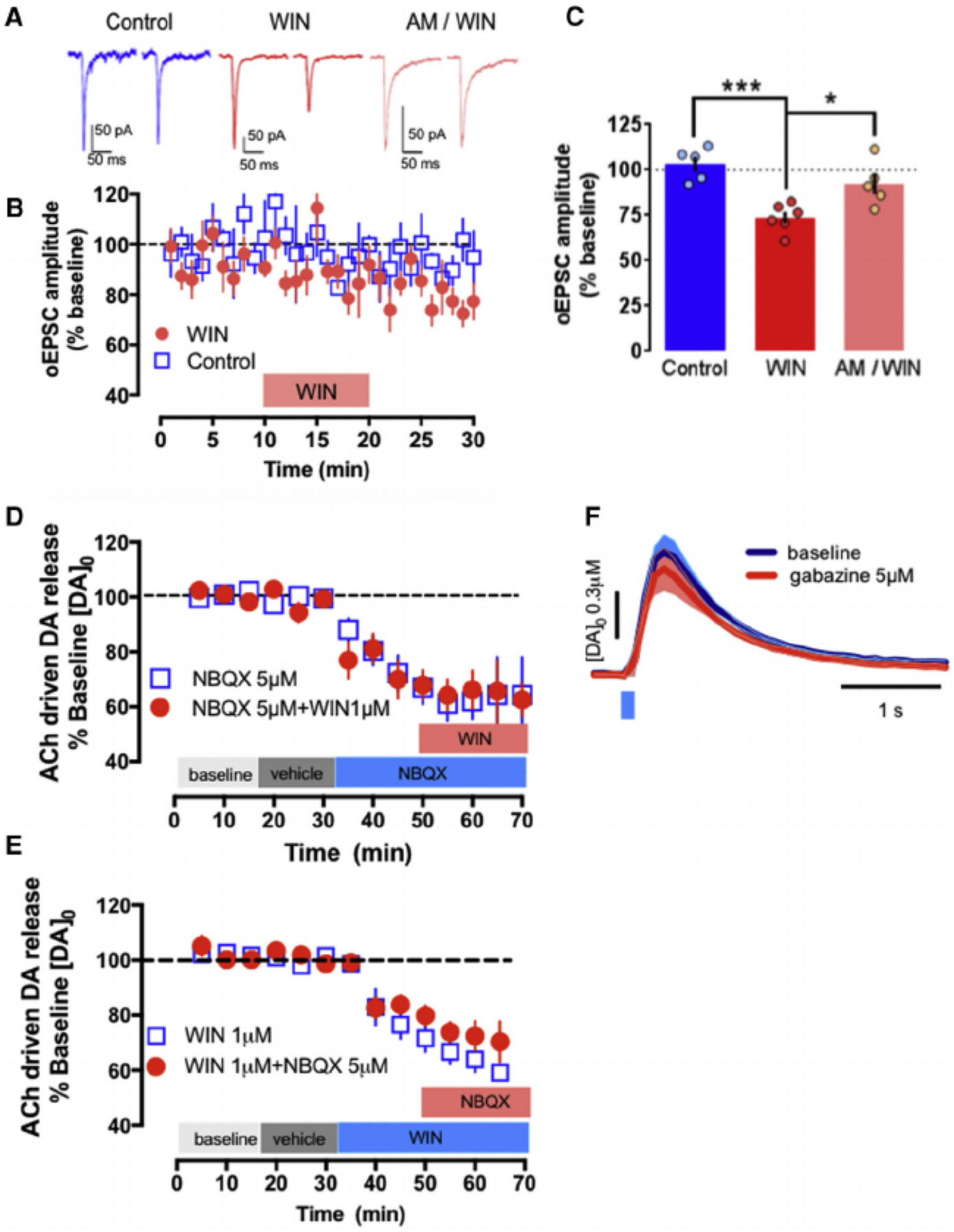

Figure 2. CB1 Receptor Modulation of DA Release Driven by Cholinergic Interneurons Requires Glutamatergic Transmission

(A–E) CB1 receptor activation decreases the amplitude of excitatory postsynaptic currents (EPSCs) elicited by activation of cholinergic interneurons (CINs). Representative traces (A) and summary data (B and C) demonstrating that 470 nm light stimulation of CINs produced measureable EPSCs recorded in MSNs. Light alone (control) did not produce a decrease in oEPSC magnitude (n = 5, p > 0.05 versus baseline). The CB1 receptor agonist, WIN55,212-2 (1 M; WIN) decreased the magnitude of EPSCs (n = 6; p < 0.001 versus Control) and this effect was blocked by the CB1 receptor antagonist AM251 (3 M AM251; WIN + AM251; n = 5; p < 0.05 versus WIN; p > 0.05 versus Control). Representative traces are the average of the first 10 min (first of each pair) and the final 10 min (second of each pair) of recording and statistical analyses were performed on these same time windows. Scale bars represent 50 pA, 50 ms. All error bars indicate SEM. Optically activated CINs elicit a significant increase in DA release that is decreased in the presence of the AMPA receptor antagonist, NBQX (5 M; D and E). Co-application of WIN does not decrease DA levels further when applied in the presence of NBQX (D and E).

(F) Gabazine did not significantly modify CIN-driven DA release in the nucleus accumbens. Blue rectangles (not to scale) represent time of optical stimulation.

All data are expressed as mean ± SEM.

application of WIN (1 M) reduced the amplitude of recorded MSN oEPSCs (Figures 2A–2C; reduction to 74% ± 3% baseline). When AM251 (3 M) was present throughout the recording, application of WIN no longer decreased MSN oEPSC amplitude (Figures 2A–2C; 92% ± 6% baseline), demonstrating that the effect of WIN occurs through CB1 receptor activation. To determine whether AMPA and CB1 receptors share a common neural substrate underlying the effects of WIN on CIN-driven DA release, we utilized a combined pharmacological and voltammetric approach. To achieve this, we initially activated CINs optogenetically and elicited a significant decrease in DA release in the presence of the AMPA receptor antagonist, NBQX (5 M; Figure 2D), as in our prior publication (Cachope et al., 2012). The effects of NBQX were recapitulated with the use of the non-competitive AMPA receptor antagonist GYKI 52466 (Figure S3B). Next, we observed that application of WIN did not decrease DA levels further when applied in the presence of NBQX (Figure 2D). We also observed this same effect when NBQX was applied in the presence of WIN (Figure 2E). This occlusion of the effect of WIN by NBQX suggests that CB1 receptors are localized upstream of AMPA effector sites.

Consistent with previous reports (Sidló et al., 2008), we also found that DA release evoked by single pulse electrical stimulation was unaffected by WIN (Figures S3C and S3D) in agreement with a lack of CB1 receptor expression on dopaminergic terminals within the NAc. Interestingly, AMPA receptors are similarly uninvolved in DA release induced by single electrical pulses (Avshalumov et al., 2003). These findings indicate that

(D) Average (±SEM) CIN-driven DA release recorded *in vitro* following single pulse optical stimulation was similarly decreased by WIN (left panel, n = 7) and the decrease was blocked by AM251, a CB1 receptor antagonist (right panel, n = 5).

(E) Time course of peak CIN-driven $[DA]_O$ showing the effect of WIN (1 M, red trace; $F_{(12,90)} = 31.27$; $p < 0.0001$).
(F) Time course showing that pretreatment with AM251 (3 M, red trace, n = 5) prevents the reduction elicited by WIN (1 M) on DA levels elicited by optical stimulation of CINs. Blue rectangles (not to scale) represent time of optical stimulation.

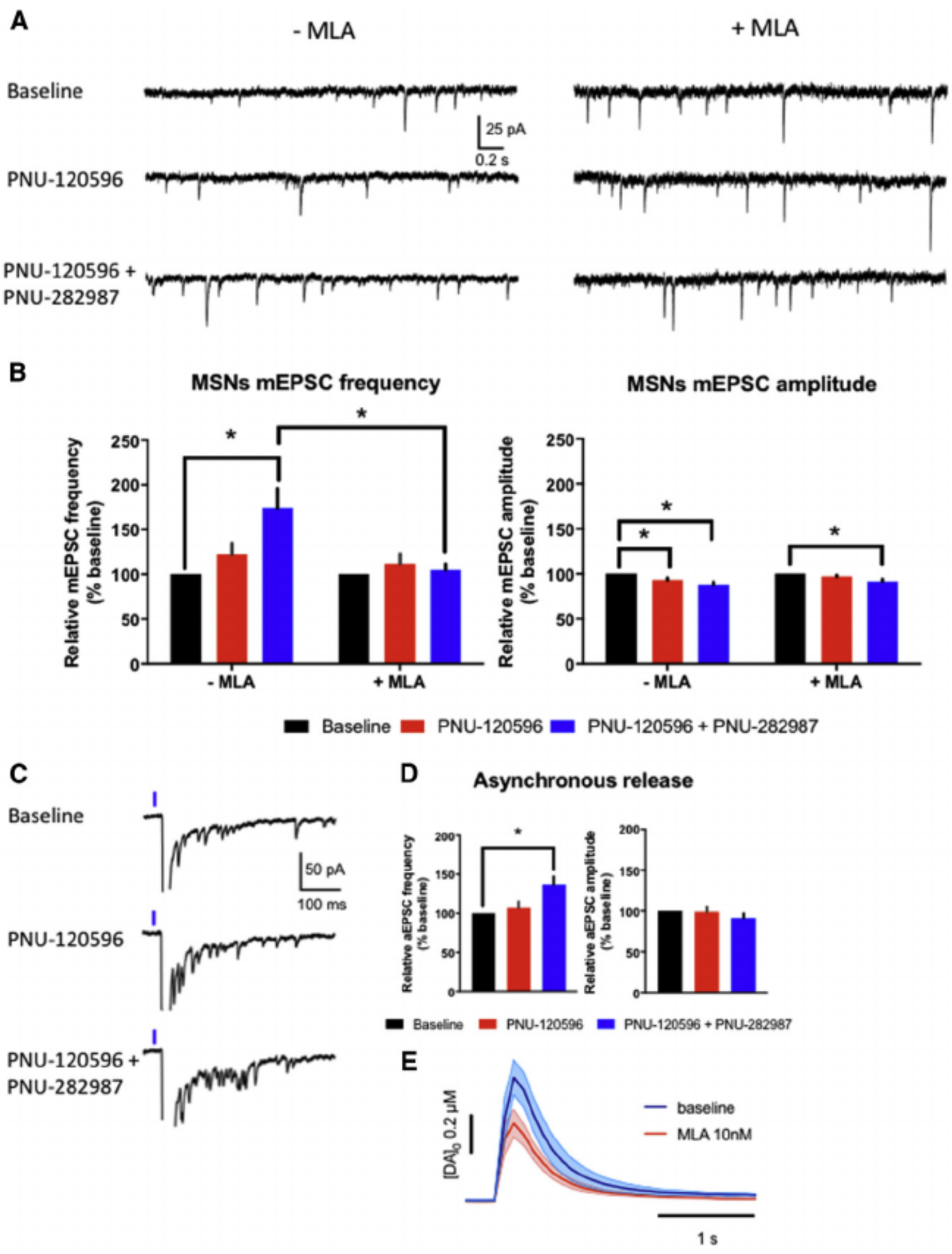

Figure 3. Nicotinic Acetylcholine Receptors Stimulate Glutamatergic Transmission Presynaptically in the Nucleus Accumbens

(A and B) The effect of pharmacological activation of 7 nAChRs on mEPSCs recorded from MSNs in C57BL/6J mice was evaluated. Sample traces showing recordings (A) and summary data (B) for mEPSC frequency and amplitude following a 5 min baseline, application of the 7-selective positive allosteric modulator (PAM) PNU-120596 (10 M), and additional 5 min of co-application of the PAM and the 7-selective agonist PNU-282987 (500 nM). Recordings were performed in the absence or presence of the 7 antagonist methyllycaconitine (MLA, 100 nM). Main effect of PAM/agonist treatment ($F_{(2,36)} = 8.747$, $p = 0.0008$), a main effect of antagonist treatment [$F_{(1, 18)} = 5.213$, $p = 0.0348$], and a significant interaction between PAM/agonist and antagonist treatments ($F_{(2,36)} = 7.745$, $p = 0.0016$) were observed. Post hoc Bonferroni comparisons demonstrated that the combination of PAM and the agonist significantly increased mEPSC frequency compared to baseline (174.5% ± 21.5%).
(C) Representative traces showing asynchronous glutamate release.
(D) Asynchronous glutamate release was evoked by optical stimulation of ChR2-expressing mPFC terminals. Baseline frequencies and amplitudes were averaged over the full 5-min period, and PAM and agonist effects were measured for 3 and 4 min of each drug application. There was a significant effect of drug treatment on frequency ($F_{(2,23)} = 10.06$, $p = 0.0027$) but not amplitude ($F_{(2,23)} = 1.441$, $p = 0.2705$).
(E) Optical acetylcholine driven DA release was significantly inhibited by application of MLA (10 nM) ($p < 0.001$; $t = 6.17$, $df = 8$; $n = 9$).
All data are expressed as mean ± SEM.

glutamatergic contributions to DA release and CB1 receptor modulation of release differ when release is driven by electrical stimulation versus direct CIN activation. A possible contribution of GABA to regulation of CIN-evoked DA release was ruled out because bath application of gabazine, a $GABA_A$ receptor antagonist, (5 M) did not change DA release induced by optical CIN activation (Figure 2F).

Nicotinic Acetylcholine Receptors Stimulate Glutamatergic Transmission Presynaptically in the Nucleus Accumbens

Previous reports suggest that activation of presynaptic 7-containing nAChRs can facilitate glutamate release in the NAc

hypothesis, we examined the effect of pharmacological activation of 7 nAChRs on mEPSCs recorded from MSNs in C57BL/6J mice. Following a 5-min baseline recording, the 7-selective positive allosteric modulator (PAM) PNU-120596 (10 M) was bath applied for 5 min, followed by an additional 5 min of co-application of the PAM and the 7-selective agonist PNU-282987 (500 nM) (Figure 3A). Recordings were performed in the absence or presence of the 7 antagonist methyllycaconitine (MLA, 100 nM). Two-way repeated-measures ANOVA analysis of mEPSC frequency revealed a main effect of PAM/agonist treatment ($p < 0.001$), a main effect of antagonist treatment ($p < 0.05$), and a significant interaction between PAM/agonist and antagonist treatments ($p < 0.01$) (Figure 3B). Post hoc Bonferroni comparisons demonstrated that the combination of PAM and the agonist significantly increased mEPSC frequency compared with baseline (175% ± 22%).

(Jones et al., 2001; Kaiser and Wonnacott, 2000; Zhang and Warren, 2002) and this mechanism could link CIN stimulation to glutamate release that subsequently facilitates increases in extracellular DA concentration. To examine the viability of this

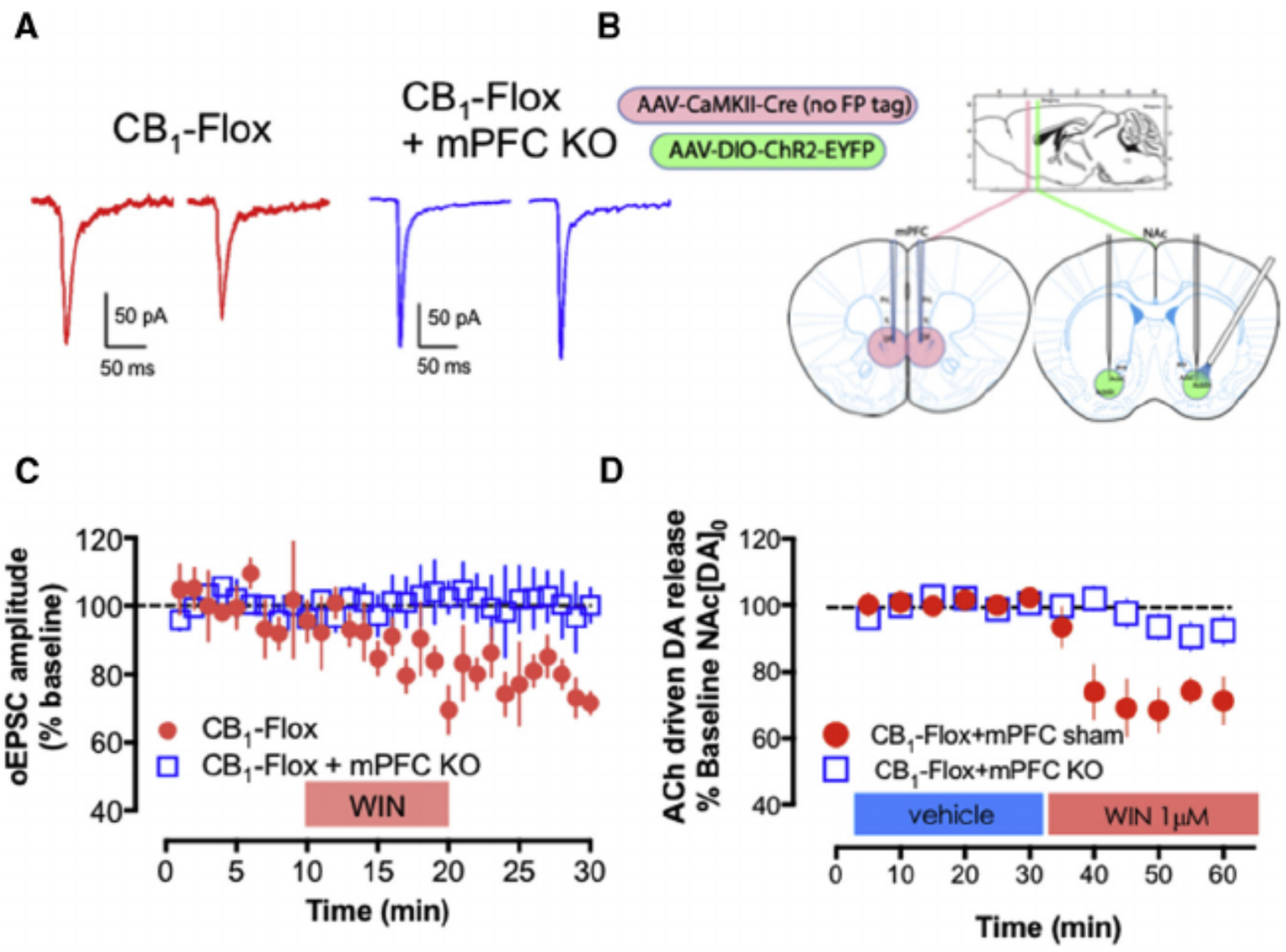

Figure 4. Conditional Deletion of CB1 Receptors on Cortical Glutamate Afferents to the Nucleus Accumbens Abolishes the Effect of WIN55,212-2 on Glutamate and DA Release Driven by Activation of Cholinergic Interneurons

(A–C) Representative traces (A) and experimental schematic (B) showing injection sites and summary data (C) demonstrating that treatment with the CB1 receptor agonist WIN55,212-2 (WIN) produces a significant decrease in the amplitude of oEPSCs in brain slices in which CB1 receptor expression was ablated in cholinergic interneurons (CINs). In mice that received an injection of a CaMKII -driven cre-recombinase viral vector into mPFC, WIN fails to induce a depression of oEPSCs. Representative traces are the average of the first 10 min (first of each pair) and the final 5 min (second of each pair) of recording and statistical analyses were performed on these same time windows. Scale bars represent 50 pA, 50 ms. All error bars indicate SEM.

(D) WIN does not decrease DA release evoked by CIN activation in CB1$^{flox/flox}$ animals transduced with the CaMKII -Cre-rAAV vector in mPFC ($n = 11$) but continues to inhibit it in animals transduced with the control CaMKII -EGFP-rAAV ($n = 4$) ($F_{(1,13)} = 8.851$; $p < 0.05$).

observe this small decrease in mEPSC amplitude over the course of control mEPSC recordings in MSNs; therefore, this result is unlikely to be related to activation of 7 nAChRs. In addition, to directly assess whether 7 nAChRs can regulate glutamate release onto CINs, we also measured mEPSC frequency from CINs with the 7 PAM accompanied by the agonist PNU-282987 and found a significant increase in mEPSC frequency (Figure S4). Lastly, to further demonstrate that mPFC terminals contain functional nicotinic receptors, we examined asynchronous glutamate release. Briefly, increased frequency of asynchronous mEPSCs would indicate a presynaptic effect, most likely an increase in probability of glutamate release, while a change in amplitude would indicate a change in postsynaptic responsiveness. For this experiment, MSNs were recorded in aCSF containing 0 mM Ca^{2+} and 4 mM Sr^{2+}. Asynchronous glutamate release was evoked by optical stimulation of ChR2-expressing mPFC terminals (Figures 3C and 3D). Repeated-measures one-way ANOVA shows significant effect of drug treatment on frequency ($p < 0.01$) but not amplitude. Post hoc Dunnett's test of frequency shows a significant increase in frequency in the PAM plus agonist condition compared with control (138% ± 10%), but no effect of PAM alone. Having found that activation of 7 nAChRs modulates excitatory synaptic transmission through changes in the probability of glutamate release, we posited that blockade of these receptors could inhibit the glutamate-dependent component of CIN-evoked DA release. Moreover, MLA inhibited the effect of the PAM/agonist on mEPSC frequency (Figures 3A and 3B). We also observed a small but statistically significant decrease in mEPSC amplitude that was not inhibited by MLA (Figure 3B). We commonly

Conditional Deletion of CB1 Receptors on Cortical Glutamate Afferents to the Nucleus Accumbens Curtails CB1 Receptor Agonist-Mediated Decreases in CIN-Evoked DA Release

To better understand the contribution of cortical glutamatergic afferents to the inhibitory effects of WIN on CIN-evoked DA release in the NAc, we used the ChAT::cre/CB1$^{flox/flox}$ mice described above. We confirmed that light activation of CINs produced oEPSCs recorded in MSNs and that treatment with WIN still elicited a decrease in the amplitude of oEPSCs (78% ± 3% of baseline; in these animals (Figures 4A and 4C). Next, we used a cre-recombinase-driven approach to delete CB1 receptors in cortical pyramidal projections neurons of ChAT::cre/CB1$^{flox/flox}$ mice. Specifically, these mice were transduced with a recombinant AAV vector encoding cre (or EGFP as a control) under the control of the CaMKII promoter into the mPFC (Chiarlone et al., 2014) (Figure 4B). This treatment selectively ablates the CB1 protein on cortical projection neurons, including those projections to the NAc (Chiarlone et al., 2014). Experiments were initiated at least 7 weeks following transduction to allow for deletion of CB1. The amplitude of oEPSCs was unchanged by WIN (100% ± 9% of baseline) in brain slices from ChAT::cre/CB1$^{flox/flox}$ mice transduced with the CaMKII -Cre-rAAV vector in mPFC (Figures 4A–4C). Additionally, WIN no longer decreased CIN-evoked DA release ($n = 11$) when animals were transduced with the CaMKII -Cre-rAAV vector in mPFC

indeed, the application of MLA at a concentration that has selectivity for 7 versus other nAChR subtypes (10 nM, Mogg et al., 2002) significantly inhibited CIN-driven DA release ($p < 0.001$, Figure 3E). These results suggest that functional nicotinic receptors exist on prefrontal glutamate terminals and augment DA release.

but still inhibited DA release in animals transduced with the control CaMKII -EGFP-rAAV vector ($n = 4$) ($p < 0.0001$; Figure 4D). These data suggest that optical CIN stimulation recruits CB1 receptor-expressing glutamatergic afferents that enhance DA release and that CB1 activation modulates these glutamatergic afferents.

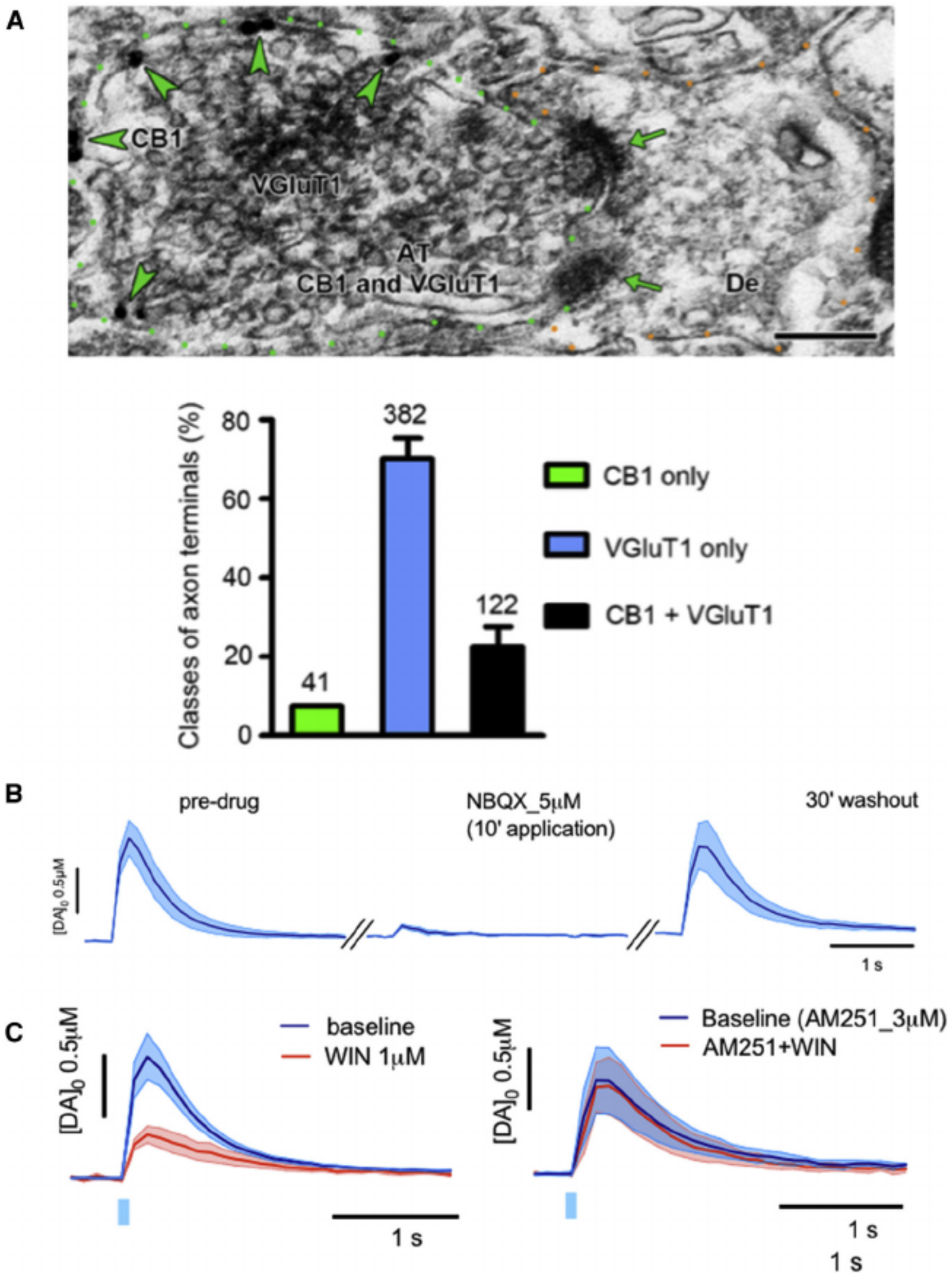

Figure 5. Selective Activation of Excitatory Prefrontocortical Projections to the Nucleus Accumbens Enhances DA Release and Is Modulated by Cortical CB1 Receptors

(A) In the nucleus accumbens, axon terminals (AT, green outline) co-expressing CB1 (gold particles, green arrowheads) and VGluT1 (scattered dark material) made asymmetric synapses (green arrows) with a dendrite (De, orange outline). Scale bar represents 200 nm. Bottom panel shows quantification of the different classes of axon terminals observed.

(B) C57BL/6J mice were transduced with a recombinant AAV vector under the control of the CaMII promoter into the mPFC (AAV1.CamKIIa. hChR2(II134R)-eYFP; blue trace). Single light pulse activation of mPFC afferents in the nucleus accumbens elicits DA release ($n = 6$), which is prevented by NBQX.

(C) When the CB1 receptor agonist, WIN55,212-2 (WIN) was added to the slice, a marked reduction in cortically evoked DA release was observed (red trace, approximately 60%, $p < 0.0001$; $n = 4$), an effect blocked in the presence of the CB1 receptor antagonist AM251. Blue rectangles (not to scale) represent time of optical stimulation.

All data are expressed as mean ± SEM.

AMPA Receptor Activation on Accumbal DA Terminals Elicits DA Release

One mechanism that could underlie the above findings would be that glutamate release from cortical terminals directly depolarizes dopaminergic axons. To test this, we initially prepared coronal brain sections for immunohistochemical analysis, which revealed that the GluA1 and A2 subunits of the AMPA receptor are clearly detectable within tyrosine hydroxylase (TH)-positive axons in the NAc (Figure S5A, top). To validate these findings, this manipulation produced robust levels of DA release (Figure S5B, left) compared to micro-pressure-applied aCSF (Figure S5B, right).

Excitatory Prefrontocortical Projections to the Nucleus Accumbens Enhance DA Release and Are Modulated by Cortical CB1 Receptors

Given the absence of CB1 receptors on CINs and DA axons, as discussed above, another site for CB1 regulation of CIN-evoked DA release could be glutamatergic afferents from mPFC. We verified that CB1 receptors were expressed on mPFC glutamate afferents in the NAc by examining terminals expressing the vesicular glutamate transporter type I (VGlut1, a protein mainly found on cortical afferents) using immuno-electron microscopy. Dense expression of the CB1 receptor was detected in approximately one quarter of the VGlut1 axon terminals (Figure 5A). In light of our data suggesting that activation of AMPA receptors contributes to DA release (Figure S5B), including a contribution following CIN activation (Figures 2D and 2E), we sought to deter-

we performed immuno-electron microscopy analysis of accumbal tissue and confirmed that AMPA receptors are indeed located on the longitudinal axis of DA terminals (Figure S5A, bottom). To further determine whether depolarization of DA terminals by AMPA receptor activation is sufficient to induce DA release, we micro-pressure applied AMPA (100 M) onto slices from C57BL/6J mice in the presence of TTX (100 nM).

mine whether this could be achieved by cortically released glutamate as well. Specifically, we transduced C57BL/6J mice with a recombinant AAV vector expressing ChR2 under the control of the CaMKII promoter injected into the mPFC. Seven weeks after transduction, NAc brain slices were prepared for voltammetric recordings. Single light pulse activation of mPFC afferents in the NAc elicited DA release, which was tetrodotoxin (TTX)

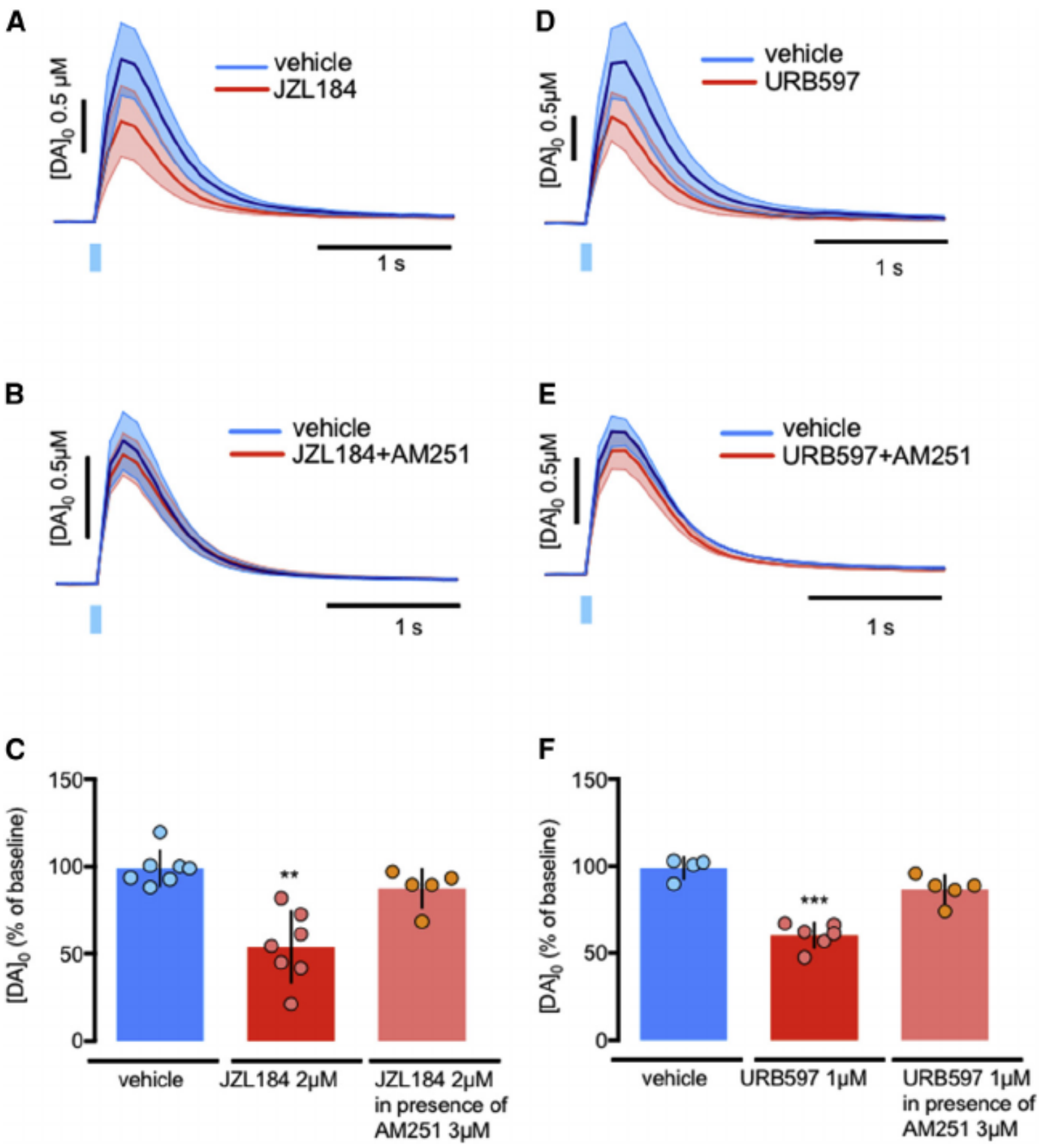

Figure 6. Raising Tissue Levels of Endogenous Cannabinoids Mimics the Effect of Full CB1 Receptor Agonism

(A and B) The monoacylglycerol lipase inhibitor JZL184 (2 M) decreases DA release evoked by activation of cholinergic interneurons (CINs). Voltammetric average traces showing the effect of 35 perfusion of JZL184 without blocking CB1 receptors (A; $p < 0.001$; $t = 5.246$, $df = 12$; $n = 7$) and pretreating slices with the CB1 receptor antagonist AM251 at 3 M (B; $n = 6$).

(C) Average data for JZL184 and AM251 (**$p < 0.001$).

(D) Raising tissue levels of anandamide with URB597 (1 M), a FAAH inhibitor, similarly decreased DA release evoked by CINs ($p < 0.0001$; $t = 8.753$, $df = 8$).

(E) Pretreatment with AM251 (3 M) blocked the decrease of DA release induced by URB595.

(F) Average data for URB597 and AM251 (***$p < 0.0001$). Blue rectangles (not to scale) represent time of optical stimulation.

All data are expressed as mean ± SEM.

sensitive ($n = 6$; Figures S6A and S6B), suggesting that glutamatergic inputs from cortical terminals indeed drive DA release in the NAc in support of recent work (Kosillo et al., 2016). Application of NBQX (5 M) for 10 min significantly decreased DA release evoked by optogenetic stimulation of PFC afferents (90%). Following a 30-min washout period, DA signals recovered (Figure 5B). Previous work suggests that cortically driven DA release is mediated by activation of CINs (Kosillo et al., 2016). In an attempt to isolate the effects of ChR2-expressing mPFC inputs directly to dopaminergic terminals, we added 4-aminopyridine (4-AP, 100 M) following TTX (100 nM). TTX prevents synaptic transmission, and 4-AP is used to allow more efficient ChR2-mediated depolarization of axonal and presynaptic membranes. This technique has been used in past studies to isolate monosynaptic responses driven by ChR2 activation (Cruikshank et al., 2010; Petreanu et al., 2007). Application of TTX for

facilitation of DA release induced by 4 2 nicotinic receptors may occur in the absence of action potential generation, similar to what we observed following pressure application of AMPA. Of course, this new finding indicates that the TTX/4-AP procedure did not isolate a truly monosynaptic response contrary to our initial plans, and additional work is needed to determine the mechanisms underlying the ACh role in PFC-stimulated release under these conditions. Nonetheless, these data support the idea that PFC-induced DA release requires the activity of CINs.

We next aimed to functionally probe the role of CB1 receptors on cortical afferents. To do this, we bath applied WIN (1 M) and observed a marked reduction of cortically evoked DA release (approximately 60%; $n = 4$; Figure 5C, left). Moreover, the actions of WIN were completely prevented by addition of the CB1 receptor antagonist AM251 (3 M) (Figure 5C, right). Therefore, PFC-driven NAc DA release is modulated presynaptically by CB1 receptors and glutamatergic synaptic transmission onto CINs is similarly modulated through CB1 receptor-mediated regulation as shown in Figure S7.

Raising Tissue Levels of Endogenous Cannabinoids

6–12 min blocked selective mPFC terminal ChR2-evoked DA responses completely. Addition of 4-AP for 6 min (during TTX application) allowed for laser-evoked responses to recover (Figures S6C–S6E). Somewhat surprisingly, these responses were still sensitive to blockade by 4 2-containing nAChR receptor antagonist (Figures S6D and S6E), consistent with the findings of Kosillo et al. (2016) in the absence of TTX. Thus, our observations extend these previous findings by providing evidence that

Mimics the Effect of WIN55,212-2

Because exogenous activation of CB1 receptors modulates cortical and glutamate-sensitive CIN-evoked DA release, we next investigated whether raising tissue levels of eCBs would elicit inhibitory effects similar to those observed with WIN. Signaling by the eCB 2-AG, one of the better-characterized eCBs released from membrane phospholipid precursors, is metabolically regulated by its degradative enzyme,

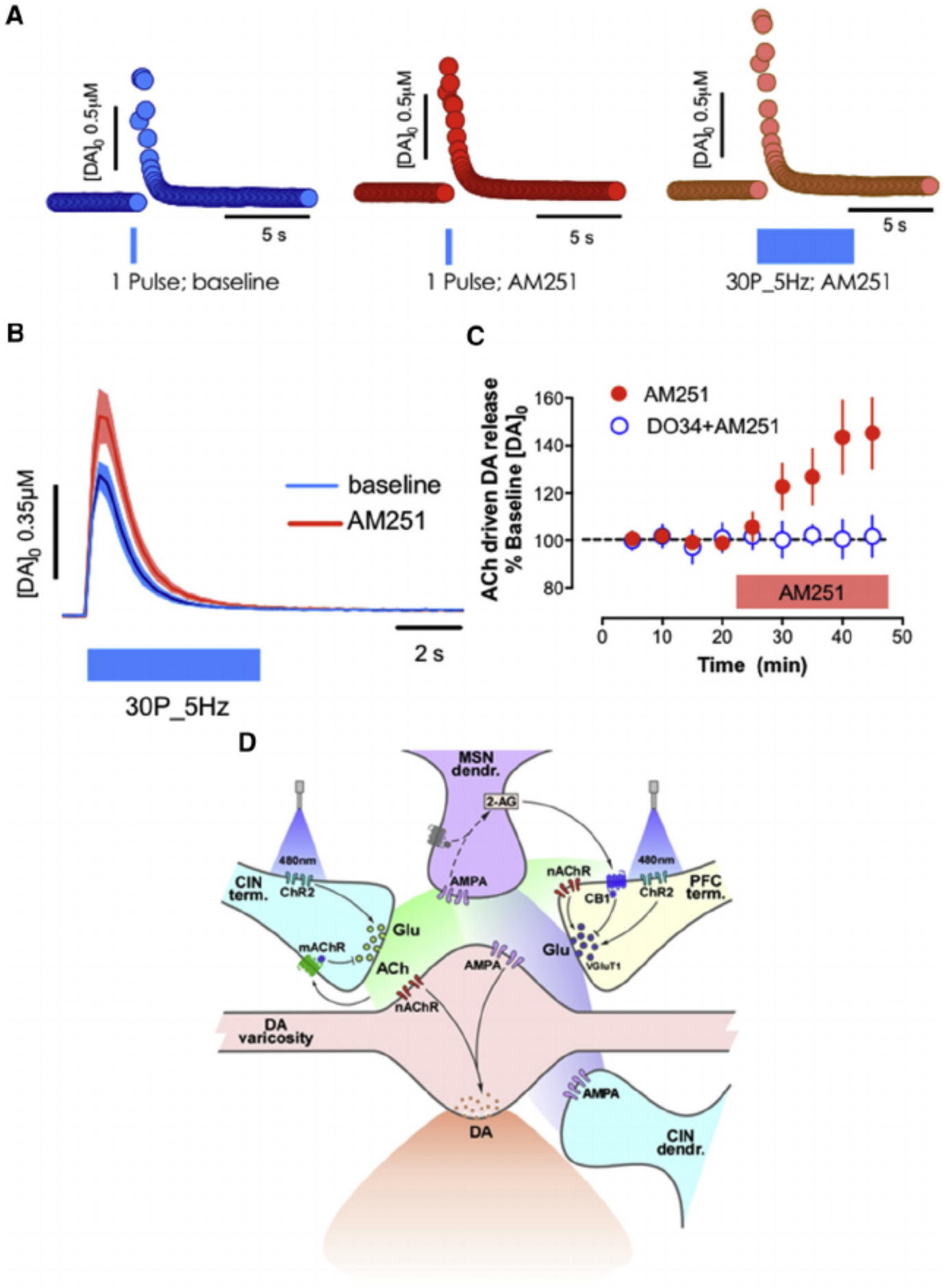

Figure 7. "On-Demand" Synthesis of 2-AG Occurs following the Delivery of Optical Trains to Cholinergic Interneuron

(A–C) Concentration traces (A) for DA release triggered by single pulse optical stimulation of cholinergic interneurons (CINs), pre-drug (left panel), in the presence of the CB1 receptor antagonist AM251 (3 M) (middle panel), and following optical trains of 30 pulses at 5 Hz in presence of AM251 (right panel). Optical train stimulation of CINs increases DA release in presence of AM251 (A and B). The AM251-induced increase in DA release was completely abolished in the presence of the diacylglycerol lipase inhibitor, DO-34 (1 M) ($F_{(1,14)} = 8.246$; $p < 0.05$; $n = 8$) (average traces, B, and time course, C). Blue rectangles (not to scale) represent time of optical stimulation.

(D) Working model for the role of accumbal CB1 receptors expressed on cortical afferents in the terminal regulation of phasic DA release. The cartoon illustrates how glutamatergic and cholinergic transmission drives nucleus accumbens DA release and its regulation by activation of CB1 receptors expressed by mPFC terminals in the nucleus accumbens. For cholinergic interneuron (CIN)-induced DA release, the first event that occurs is optogenetic depolarization of CINs; this leads to ACh and glutamate release from this cell population. Our data show that ACh release (the main diffusible component of this stimulation) can directly drive mPFC terminals via activation of nicotinic receptors. This leads to increased glutamate release that further drives both CINs and possibly also AMPARs on DA terminals. CIN activation also leads to DA release via the known nAChR response on DAergic terminals, and this is likely boosted by the ACh activation of glutamate release from mPFC terminals that further drives CIN activity. The activation of glutamatergic terminals accounts for the sensitivity of DA release to CB1 activation (the only cellular location where CB1 and eCBs could affect this circuit). This scenario also accounts for the observation that AMPAR antagonists inhibit CIN-induced DA release, as glutamate released from PFC afferents likely participates in driving CIN activity (and is likely to also drive DA release more directly under experimental conditions different than those from our *in vitro* recordings). When DA release is evoked by direct optogenetic PFC terminal activation, the primary target of this stimulation is the CIN population. Here again, DA release evoked by PFC terminal stimulation is modulated by CB1 receptors located on these terminals.

All data are expressed as mean ± SEM.

monoacylglycerol lipase (MAGL). Thus, we used the MAGL inhibitor JZL184 (2 M) to raise tissue levels of 2-AG. When the NAc. To this end, we used URB597, an inhibitor of fatty acid amide hydrolase (FAAH) the primary degradative enzyme for

JZL184 was bath applied, DA levels evoked by single pulse CIN optical stimulation were reduced by 46% ± 8% ($p < 0.001$; $n = 7$; Figures 6A and 6C). When slices were pretreated with the CB1 receptor antagonist AM251 (3 M) for 45 min and the antagonist was then bath applied together with JZL184, the reduction elicited by JZL184 was prevented (Figures 6B and 6C). We next determined whether anandamide, another eCB released under specific conditions in the striatum (Gerdeman et al., 2002; Giuffrida et al., 1999; Zhang et al., 2015), would similarly depress DA release caused by optical activation of CINs in anandamide. Addition of URB597 to the bath decreased CIN-evoked DA release (Figures 6D and 6F) in a CB1 receptor-dependent fashion (Figures 6E and 6F). These results suggest that eCB signaling within the NAc has the potential to modulate DA release evoked by activation of CINs.

"On-Demand" Synthesis of 2-AG Occurs following the Delivery of Optical Trains to CINs

The results above show that eCBs can potentially limit CIN-evoked DA release. In our next experiments, we asked whether eCBs could actively be recruited to shape patterns of CIN-evoked DA release. 2-AG is the primary eCB that mediates retrograde synaptic signaling at central synapses (Tanimura

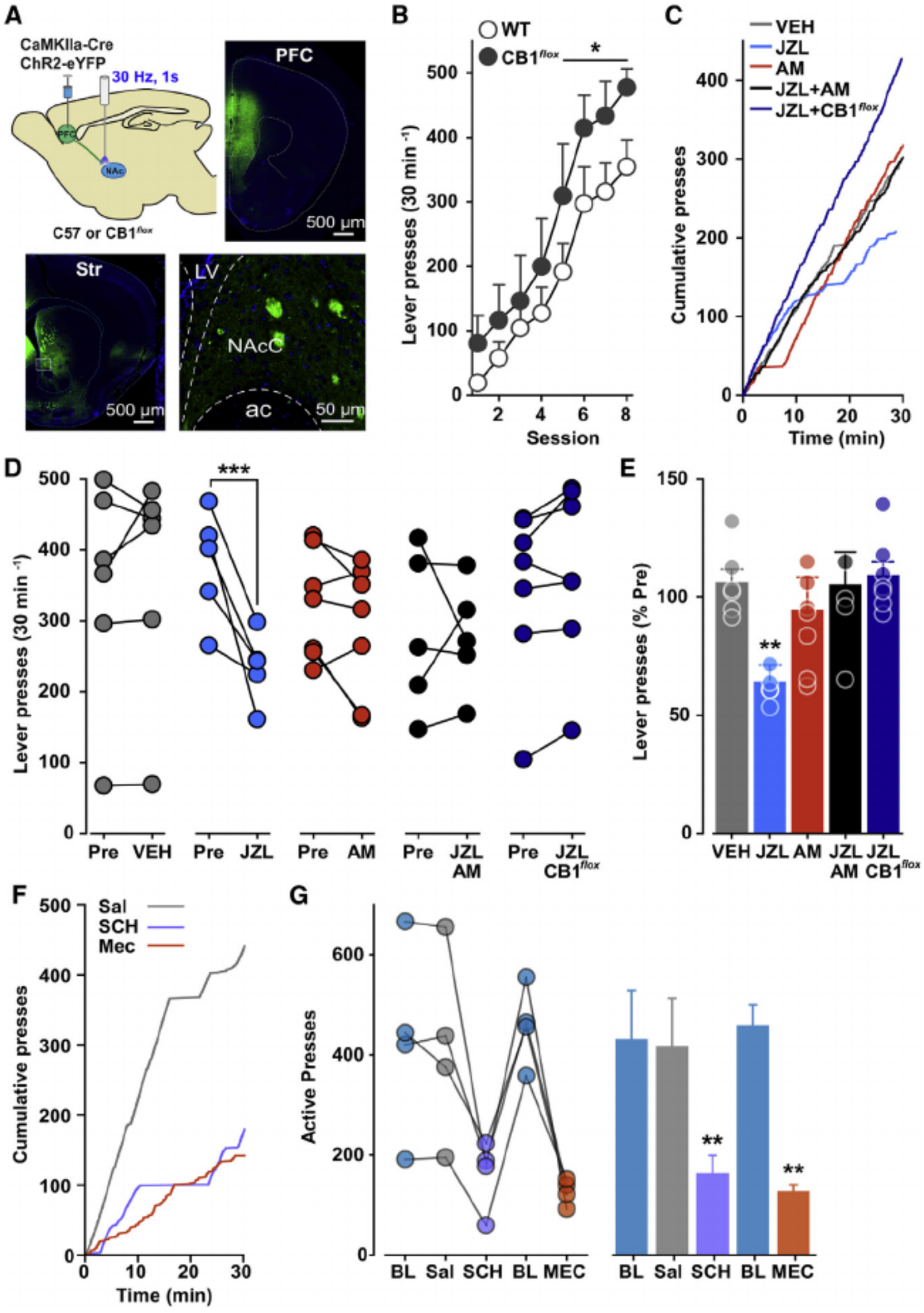

Figure 8. CB1 Receptor Activation Modulates Reinforcement Driven by Cortical Glutamate Afferents into the Nucleus Accumbens

(A) Schematic of viral transduction in the prefrontal cortex (PFC) and optic fiber placement in the striatum (Str; top, left). Fluorescent tag (eYFP; green) and DAPI (blue) in the PFC (top, right) and fibers in the NAc (bottom). LV, lateral ventricle; NAcC, NAc core; ac, anterior commissure.

(B) Conditional deletion of the CB1 receptor on PFC afferents potentiated self-stimulation (2-way repeated-measures ANOVA; session: $F_{(12,54)} = 18.57$, $p < 0.001$; group: $F_{(1,84)} = 4.90$, $p < 0.05$; group x session interaction: $F_{(7,84)} = 1.90$, $p = 0.08$).

(C) Representative cumulative response records following eCB manipulations.

(D and E) JZL-attenuated active presses compared to the prior behavioral session (Pre) when data are expressed as (D) the number of active presses (two-way repeated-measures ANOVA; drug session interaction: $F_{(4,25)} = 5.14$, $p < 0.001$) and (E) percent change (one-way ANOVA: $F_{(4, 25)} = 6.29$, $p = 0.001$). JZL effects were reversed by AM-251 (AM) and absent following conditional CB1 receptor deletion. Data are represented as mean + SEM. ***$p < 0.001$, **$p < 0.01$ (Tukey's post hoc test).

(F) The D1 receptor antagonist SCH23390 (SCH, 1 g/0.5 L) and the non-selective nACh receptor mecamylamine (MEC, 10 g/0.5 L) potently attenuate responding in ICSS when injected into the NAc compared to saline (0.5 L).

(G) Pooled behavioral effects of intracerebral administration of SCH and mecamylamine versus saline during ICSS maintained by optical stimulation of cortical terminals in the NAc (one-way repeated-measures ANOVA: $F_{(3,12)} = 10.80$, $p < 0.001$. **$p < 0.01$ versus saline).

range for CIN-evoked DA release in the NAc (Cachope et al., 2012). Under these conditions, DA release increased by 45% ($p < 0.001$; $n = 8$; Figures 7A, right, 7B, and 7C) relative to train-induced release in the absence of the antagonist. Importantly, the increase in DA release induced by AM251 was completely abolished in the presence of the DGL inhibitor DO34 (1 M; Ogasawara et al., 2016; $p < 0.05$) as depicted in Figure 7C), suggesting that applica-

et al., 2010). On-demand 2-AG biosynthesis is catalyzed by diacylglycerol lipase (DGL) via calcium- and G$_q$-protein-coupled receptor-dependent mechanisms (Tanimura et al., 2010). Here, we show that AM251 does not modify DA release in response to single pulse optical stimulation (Figure 7A), suggesting that this pattern of stimulation is not sufficient to produce 2-AG release. Therefore, to investigate the conditions better suited for 2-AG mobilization following CIN optical activation, we incubated slices with or without AM251 (3 M) and optically activated CINs with 30 pulses delivered at 5 Hz, a frequency previously shown to be in the preferential pulse tion of optical trains to CINs, but not stimulation with single pulses, mobilizes 2-AG to limit CIN-driven DA release (Figure 7D). Addition of AM251 during train stimulation prevents activation of CB1, presumably by displacing 2-AG released during stimulation. The CB1 receptors activated by 2-AG are almost certainly those on cortical terminals given our evidence that the receptor is not expressed by other relevant neurons within the circuit as shown in the diagram on Figure 7D. Through this indirect mechanism, CB1 blockade ultimately prevents 2-AG actions that would normally inhibit extracellular DA levels.

2-AG Binding to CB1 Receptors Expressed on mPFC Terminals in the Nucleus Accumbens Constrains Reinforcement Sustained by Optical Activation of These Cortical Axons

It has previously been demonstrated that optical activation of cortical terminals in the NAc reinforces instrumental behavior (Britt et al., 2012). Here, we assessed whether CB1 receptors influence reinforcement driven by mPFC glutamate afferents in the NAc. Specifically, we measured self-stimulation induced by optogenetic activation of ChR2-expressing accumbal mPFC axons (Figure 8A; Britt et al., 2012) and its sensitivity to eCBs, DA, and nACh receptor manipulations. We observed robust self-stimulation behavior (Figure 8B) as previously described (Britt et al., 2012). Conditional knockout of the CB1 receptor on PFC afferents potentiated self-stimulation compared to controls, supporting the idea that eCB signaling can modulate functional effects of PFC activation *in vivo* (Figure 8B and Figure S8). Conversely, self-stimulation was attenuated by increasing tissue levels of the eCB 2-AG by inhibiting its degradation with JZL184 (18 mg/kg, i.p.). Moreover, the effects of JZL184 were reversed by co-administration of AM251, which did not have any effects per se at the relatively low dose we used (0.75 mg/kg. i.p., Figures 8C–8E). The effects of JZL184 were abolished in mice lacking CB1 receptors on PFC terminals (Figures 8C–8E), an effect that cannot be explained by an indiscriminate higher rate of lever pressing in animals with an ablation of CB1 receptors on PFC terminals (Figure S8). Altogether, these data suggest that this population of receptors mediates the pharmacological effects of JZL. Next, we demonstrate a link between self-stimulation of cortical terminals in the NAc and D1 receptors as shown previously by our group and others; namely, a decrease in the vigor of self-stimulation behavior induced by a D1-like receptor antagonist (Figure 8; Nowend et al., 2001; Yun et al., 2004; Cheer et al., 2007). D1 receptors were targeted, with a D1 antagonist (SCH 23390), because of their low-affinity state, which would be primarily tuned to the phasic, high concentration release of DA, documented here *in vitro* and *in vivo* (also see Cachope et al., 2012). Finally, behavior was also potently disrupted when the non-selective nACh receptor antagonist mecamylamine was infused bilaterally into the NAc at a concentration devoid of locomotor confounds (Collins et al., 2016), supporting an important role for these receptors on PFC-driven instrumental behavior, a finding that aligns with observations from our *in vitro* experiments and our prior work (Cachope et al., 2012).

DISCUSSION

CB1 receptor activation does not inhibit DA release following single pulse electrical stimulation as shown by others and by us here (Sidló et al., 2008; Szabo et al., 1999). Additionally, GABAergic transmission does not appear to contribute to the CIN-driven DA release, ruling out a role for the other major CB1-expressing neuronal subtype in striatum (i.e., the parvalbumin-positive fast-spiking interneurons and the MSNs themselves). Our results show a previously unseen level of specificity for actions of CB1 receptors in the terminal modulation of DA release and of behavior reinforced by specific activation of cortical glutamate terminals in the NAc (Figure 7D). These findings extend earlier work showing that CB1 receptors are powerful modulators of striatal DA release and motivated behavior due to their indirect disinhibitory actions on dopaminergic neurons in the midbrain (Cheer et al., 2000a, 2004; Lupica et al., 2004; Riegel and Lupica, 2004; Wallmichrath and Szabo, 2002).

The different neural substrates involved in DA release evoked by a single electrical versus optical pulse stimulation may be numerous, but differential involvement of glutamatergic synaptic transmission appears to be crucial to the explanation of our findings. Glutamate receptor antagonists have no effect on single pulse electrical stimulus-induced DA release (Avshalumov et al., 2003). Threlfell et al. showed no effect of an NMDA receptor antagonist plus a low concentration of an AMPA receptor antagonist on CIN-evoked DA release in dorsal striatum except when CINs are activated by thalamic inputs (Threlfell et al., 2012). In the NAc, antagonists of AMPA and NMDA ionotropic glutamate receptors inhibit DA release following CIN activation (Cachope et al., 2012). This discrepancy could be due to regional differences although a detailed pharmacological characterization of the involvement of all ionotropic glutamate receptors in DA release in both regions is warranted. Accordingly, we observed that optical CIN activation produces EPSCs in MSNs, responses regulated by CB1 receptors. Additionally, cortical glutamate drive onto CINs themselves is also regulated presynaptically by CB1 receptors. Glutamate release can be stimulated directly by activation of PFC afferents or indirectly through activation of 7 nAChRs on PFC terminals. The released glutamate could regulate DA release in at least two ways. It is known that cortical activation stimulates CINs and this enhances DA release through activation of nAChRs (Kosillo et al., 2016). This appears to be the predominant mechanism by which optogenetic PFC activation increases DA release given the sensitivity of this process to nAChR blockade (Figure S6; Kosillo et al., 2016). The AMPA receptors that we find on DA terminals may

Here we show that activation of CB1 receptors on cortical terminals decreases DA release evoked by CIN activation *in vivo* and in brain slices. It is unlikely that this reduction is due to decreased probability of ACh release involving activation of CB1 receptors present on cholinergic terminals, because our own data as well as that of others (Hohmann and Herkenham, 2000) demonstrate that CB1 mRNA is not expressed by CINs in the NAc and thus CB1 receptors do not directly modulate ACh release. Dopaminergic terminals do not express CB1 receptors (Julian et al., 2003), and thus these neurons are not the site of the CB1 receptor-mediated effects reported here. Consistent with this idea, glutamate release and subsequent AMPA receptor activation. This process may involve AMPA receptors on CINs as well as those receptors on dopaminergic terminals (Kaiser and Wonnacott, 2000; Kendrick et al., 1996; Smolders et al., 1996). Thus, CB1 receptors on glutamatergic afferents modulate DA release only under conditions where these afferents are activated and glutamate contributes to DA release. Together, these data lead us to propose that CB1 receptors on cortical glutamatergic terminals modulate DA release via mechanisms upstream of AMPA effector sites.

Because some studies have shown that AMPA receptor blockade actually enhances DA release evoked by electrical stimulation under specific conditions (Avshalumov et al., 2003), a provocative thought arises. If AMPA receptor blockade only inhibits CIN or mPFC-driven release of DA as shown in the present study, this implies that electrical stimulation recruits additional DA release mechanisms that are not AMPA receptor dependent. This idea is consistent with a recent study demonstrating that AMPA receptor blockade does not affect DA release induced by direct stimulation of VTA afferents (Zhang et al., 2015). Thus, direct activation of at least some dopaminergic terminals may bypass sensitivity to AMPA receptor activation (Zhang et al., 2015). It is also possible that electrical stimulation activates glutamatergic transmission to a degree that 7-type nAChRs cannot further influence release. Nevertheless, our findings are most consistent with the idea that CIN activation primarily evokes ACh release, which likely depolarizes nearby CB1 receptor-expressing glutamatergic terminals via volume transmission (Cachope and Cheer, 2014). Our finding that activation of 7-type nAChRs increases the frequency of glutamatergic mEPSCs as well as mPFC afferent-specific asynchronous glutamate release in the NAc is aligned with this hypothesis. Modulation of glutamate release by 7 nAChRs is also supported by previous studies showing that nAChRs on glutamate terminals powerfully enhance glutamate neurotransmission in NAc synaptosomes and slices (Jones et al., 2001; Kaiser and Wonnacott, 2000; Zhang and Warren, 2002). Single pulse optical CIN activation, as opposed to electrical stimulation, may depolarize CB1 (and nicotinic) receptor-expressing glutamatergic terminals, and glutamate released from these afferents activates AMPA receptors on CINs (and probably on DA terminals) to facilitate DA release (in addition to their direct depolarization by 2-expressing nicotinic receptors [Cachope et al., 2012; Threlfell et al., 2012]). Another possibility is that ACh has a tonic effect on glutamate also contribute to glutamatergically driven DA release, although it remains to be determined under which circumstances they play a role. When CINs are activated optogenetically, glutamate release driven by ACh could act directly on AMPARs located on DA terminals, although this will have to be determined in future studies. The other possibility is that glutamate released following CIN stimulation and subsequent 7 nAChR activation feeds back onto CINs to further enhance ACh release. This scenario, although admittedly complicated, cannot be ruled out at this time. Importantly, the finding that AMPA receptor blockade occludes the effects of WIN on CIN-evoked release is consistent with our results showing that CB1 receptors act by decreasing

mechanistic link between transduction at D2 receptors and anandamide synthesis has yet to be established. However, and in agreement with the ability of CB1 receptors to respond to both eCBs (Mathur and Lovinger, 2012), we observed that pharmacological elevation of 2-AG or anandamide mimic the inhibitory effects of WIN on CIN-evoked DA release in the NAc. We further provide evidence that 2-AG is released ''on demand'' following optical trains but not single pulse stimulation of CINs. Prevention of AM251-induced facilitation of DA release by blockade of 2-AG synthesis indicates that 2-AG is mobilized following sustained CIN depolarization and limits dopaminergic output. Given the sampling rate of FSCV, it may not be possible to precisely determine when the AM251 effect begins. However, it is known that eCB release can occur within hundreds of milliseconds (Heinbockel et al., 2005). Therefore, optical trains that mimic the physiological activity of CINs are likely to initiate the production of 2-AG (possibly by MSNs but other sources cannot be ruled out); this ''on demand'' mobilization of 2-AG can be followed by retrograde signaling onto CB1 receptors present on cortical glutamatergic terminals to lessen glutamate release probability and thus decrease overall CIN-evoked DA release. Unfortunately, due to the lack of specific anandamide synthesis inhibitors, it remains to be determined whether optical trains similarly mobilize this eCB.

Prefrontocortical glutamatergic afferents to the NAc are critical for the integration of contextual information related to the pursuit of rewards (Floresco, 2015). Moreover, this interface has been extensively studied with regard to eCB-mediated changes in synaptic plasticity, where CB1 receptor activation decreases strength of glutamatergic synapses onto accumbal MSNs (Robbe et al., 2002a, 2002b). The findings that WIN-mediated effects on CIN-evoked changes in MSN synaptic excitation and DA release are dramatically diminished in animals with a conditional deletion of CB1 receptors specifically in this projection, suggest that cholinergic and dopaminergic signals are more subtly intertwined than previously thought. Indeed, eCB tone may be a key activity-dependent mediator of release from terminals within these micro-circuits. Our behavioral results suggest that this is the case, at least when behavior is reinforced by optical activation of cortical terminals in the NAc (Britt et al., 2012). A key observation is that, under these circumstances, raising 2-AG levels shows an effect that is opposite to what we previously described for motivated behavior driven by stimulation of the midbrain (Oleson et al.,

release through α7-type nAChRs, but there is no evidence for this to date.

The eCBs anandamide and 2-AG are mobilized by receptor activation and depolarization of MSNs and they change synaptic strength depending on the particular signal necessary for eCB production (Hashimotodani et al., 2013). In particular, 2-AG synthesis is thought to arise mainly from activation of postsynaptic G_q/11-coupled receptors such as group I metabotropic glutamate receptors and M1/M3 muscarinic cholinergic receptors that recruit the activity of several phospholipases that produce diacylglycerol, the precursor for 2-AG (Narushima et al., 2007; Uchigashima et al., 2007). On the other hand, anandamide biosynthesis has been linked to D2 receptor activation (Gerdeman et al., 2002; Giuffrida et al., 1999), although the precise

2012), in strong support of the different mechanisms of action for 2-AG; e.g., inhibition of cortically driven excitation in the NAc versus disinhibition of DA neuron cell bodies in the midbrain. These opposite effects of JZL184 are likely to occur due to the different substrates utilized by 2-AG (i.e., activation of CB1 receptors on glutamate terminals in NAc versus CB1 receptors on GABA terminals in the VTA). We further show that behavior maintained by optical stimulation of PFC terminals in the NAc is reliant upon DA D1 (Yun et al., 2004; Cheer et al., 2007) and nicotinic receptors (Crespo et al., 2008; Feduccia et al., 2014), suggesting that it may recruit, at least in part, the mechanisms uncovered in our *in vitro* experiments for its maintenance. It is notable that nicotinic receptor blockade can, under different experimental conditions, enhance behavior

as well as phasic DA concentrations in the NAc (Collins et al., 2016), thereby highlighting a precise level of influence of these neurotransmitters that is critically dependent on the neural mechanisms that motivate instrumental behavior. Thus, a possible function of eCB signaling at PFC to NAc synapses when cholinergic activity is elevated, for example when rewards are obtained (Joshua et al., 2008), may be to promote the selection of goal-directed actions toward available reinforcers in a context- and neural substrate-specific manner. These findings are relevant to neuropsychiatric conditions where aberrant responses to contextual triggers are observed clinically, as is the case of relapse to drug seeking.

STAR METHODS

Detailed methods are provided in the online version of this paper and include the following:

- KEY RESOURCES TABLE
- CONTACT FOR REAGENTS AND RESOURCE SHARING
- EXPERIMENTAL MODEL AND SUBJECT DETAILS
  - Animals
- METHOD DETAILS
  - Stereotaxic virus injection
  - *In vivo* optical stimulation and fast-scan cyclic voltammetry
  - *In vitro* optical stimulation and fast-scan cyclic voltammetry
  - Electrophysiology
  - *In situ* hybridization and ChAT immunolabeling
  - Fluorescence microscopy and image analysis for immunodetection of AMPA receptors on DA terminals
  - Electron microscopy
  - Behavioral experiments
- QUANTIFICATION AND STATISTICAL ANALYSIS
  - Data analysis for immunohistochemistry
  - Ultrastructural analysis of brain tissue

SUPPLEMENTAL INFORMATION

Supplemental Information includes eight figures and can be found with this article online at https://doi.org/10.1016/j.neuron.2017.11.012.

Received: September 6, 2016
Revised: April 8, 2017
Accepted: November 9, 2017
Published: December 6, 2017

REFERENCES

Atwood, B.K., Kupferschmidt, D.A., and Lovinger, D.M. (2014). Opioids induce dissociable forms of long-term depression of excitatory inputs to the dorsal striatum. Nat. Neurosci. *17*, 540–548.

Avshalumov, M.V., Chen, B.T., Marshall, S.P., Peña, D.M., and Rice, M.E. (2003). Glutamate-dependent inhibition of dopamine release in striatum is mediated by a new diffusible messenger, H2O2. J. Neurosci. *23*, 2744–2750.

Britt, J.P., Benaliouad, F., McDevitt, R.A., Stuber, G.D., Wise, R.A., and Bonci, A. (2012). Synaptic and behavioral profile of multiple glutamatergic inputs to the nucleus accumbens. Neuron *76*, 790–803.

Cachope, R., and Cheer, J.F. (2014). Local control of striatal dopamine release. Front. Behav. Neurosci. *8*, 188.

Cachope, R., Mateo, Y., Mathur, B.N., Irving, J., Wang, H.L., Morales, M., Lovinger, D.M., and Cheer, J.F. (2012). Selective activation of cholinergic interneurons enhances accumbal phasic dopamine release: setting the tone for reward processing. Cell Rep. *2*, 33–41.

Cheer, J.F., Kendall, D.A., and Marsden, C.A. (2000a). Cannabinoid receptors and reward in the rat: a conditioned place preference study. Psychopharmacology (Berl.) *151*, 25–30.

Cheer, J.F., Marsden, C.A., Kendall, D.A., and Mason, R. (2000b). Lack of response suppression follows repeated ventral tegmental cannabinoid administration: an in vitro electrophysiological study. Neuroscience *99*, 661–667.

Cheer, J.F., Wassum, K.M., Heien, M.L., Phillips, P.E., and Wightman, R.M. (2004). Cannabinoids enhance subsecond dopamine release in the nucleus accumbens of awake rats. J. Neurosci. *24*, 4393–4400.

Cheer, J.F., Aragona, B.J., Heien, M.L., Seipel, A.T., Carelli, R.M., and Wightman, R.M. (2007). Coordinated accumbal dopamine release and neural activity drive goal-directed behavior. Neuron *54*, 237–244.

Chiarlone, A., Bellocchio, L., Blázquez, C., Resel, E., Soria-Gómez, E., Cannich, A., Ferrero, J.J., Sagredo, O., Benito, C., Romero, J., et al. (2014). A restricted population of CB1 cannabinoid receptors with neuroprotective activity. Proc. Natl. Acad. Sci. USA *111*, 8257–8262.

Collins, A.L., Aitken, T.J., Greenfield, V.Y., Ostlund, S.B., and Wassum, K.M. (2016). Nucleus accumbens acetylcholine receptors modulate dopamine and motivation. Neuropsychopharmacology *41*, 2830–2838.

Crespo, J.A., Stockl, P., Zorn, K., Saria, A., and Zernig, G. (2008). Nucleus accumbens core acetylcholine is preferentially activated during acquisition of drug- vs food-reinforced behavior. Neuropsychopharmacology *33*,

AUTHOR CONTRIBUTIONS

Y.M., K.A.J., B.K.A., H.W., D.P.C., I.G., and S.Z. conceived and performed experiments; Y.M., K.A.J., B.K.A., D.P.C., J.F.C., and D.M.L. wrote the manuscript; J.F.C., D.M.L., and M.M. conceived experiments and secured funding; L.B. and M.G. provided viral reagents; R.C. and M.M. provided expertise and feedback.

ACKNOWLEDGMENTS

We acknowledge funding from the Division of Intramural Clinical and Biological Research of NIAAA, ZIA AA000416 (Y.M., B.K.A., K.A.J., and D.M.L.), the Intramural Research Program of NIDA ZIA DA000511 (H.W., S.Z., and M.M.), the Spanish Ministerio de Economía y Competitividad (grant number SAF2015-64945-R to M.G.), NIH grant numbers DA022340 and DA042595 (J.F.C.) and DA041827 (D.P.C.) and a Postdoctoral Research Associate (PRAT) Fellowship from NIGMS (K.A.J.).

3213–3220.

Cruikshank, S.J., Urabe, H., Nurmikko, A.V., and Connors, B.W. (2010). Pathway-specific feedforward circuits between thalamus and neocortex revealed by selective optical stimulation of axons. Neuron *65*, 230–245.

Floresco, S.B. (2015). The nucleus accumbens: an interface between cognition, emotion, and action. Annu. Rev. Psychol. *66*, 25–52.

Feduccia, A.A., Simms, J.A., Mill, D., Yi, H.Y., and Bartlett, S.E. (2014). Varenicline decreases ethanol intake and increases dopamine release via neuronal nicotinic acetylcholine receptors in the nucleus accumbens. Br. J. Pharmacol. *171*, 3420–3431.

Gerdeman, G.L., Ronesi, J., and Lovinger, D.M. (2002). Postsynaptic endocannabinoid release is critical to long-term depression in the striatum. Nat. Neurosci. *5*, 446–451.

Giuffrida, A., Parsons, L.H., Kerr, T.M., Rodríguez de Fonseca, F., Navarro, M., and Piomelli, D. (1999). Dopamine activation of endogenous cannabinoid signaling in dorsal striatum. Nat. Neurosci. *2*, 358–363.

Hashimotodani, Y., Ohno-Shosaku, T., Tanimura, A., Kita, Y., Sano, Y., Shimizu, T., Di Marzo, V., and Kano, M. (2013). Acute inhibition of diacylglycerol lipase blocks endocannabinoid-mediated retrograde signalling: evidence for on-demand biosynthesis of 2-arachidonoylglycerol. J. Physiol. *591*, 4765–4776.

Heinbockel, T., Brager, D.H., Reich, C.G., Zhao, J., Muralidharan, S., Alger, B.E., and Kao, J.P. (2005). Endocannabinoid signaling dynamics probed with optical tools. J. Neurosci. *25*, 9449–9459.

Higley, M.J., Gittis, A.H., Oldenburg, I.A., Balthasar, N., Seal, R.P., Edwards, R.H., Lowell, B.B., Kreitzer, A.C., and Sabatini, B.L. (2011). Cholinergic interneurons mediate fast VGluT3-dependent glutamatergic transmission in the striatum. PLoS ONE *6*, e19155.

Hohmann, A.G., and Herkenham, M. (2000). Localization of cannabinoid CB(1) receptor mRNA in neuronal subpopulations of rat striatum: a double-label in situ hybridization study. Synapse *37*, 71–80.

Jennings, J.H., Rizzi, G., Stamatakis, A.M., Ung, R.L., and Stuber, G.D. (2013). The inhibitory circuit architecture of the lateral hypothalamus orchestrates feeding. Science *341*, 1517–1521.

Jones, I.W., Bolam, J.P., and Wonnacott, S. (2001). Presynaptic localisation of the nicotinic acetylcholine receptor beta2 subunit immunoreactivity in rat nigrostriatal dopaminergic neurones. J. Comp. Neurol. *439*, 235–247.

Joshua, M., Adler, A., Mitelman, R., Vaadia, E., and Bergman, H. (2008). Midbrain dopaminergic neurons and striatal cholinergic interneurons encode the difference between reward and aversive events at different epochs of probabilistic classical conditioning trials. J. Neurosci. *28*, 11673–11684.

Julian, M.D., Martin, A.B., Cuellar, B., Rodriguez De Fonseca, F., Navarro, M., Moratalla, R., and Garcia-Segura, L.M. (2003). Neuroanatomical relationship between type 1 cannabinoid receptors and dopaminergic systems in the rat basal ganglia. Neuroscience *119*, 309–318.

Kaiser, S., and Wonnacott, S. (2000). alpha-bungarotoxin-sensitive nicotinic receptors indirectly modulate [(3)H]dopamine release in rat striatal slices via glutamate release. Mol. Pharmacol. *58*, 312–318.

Kendrick, K.M., Guevara-Guzman, R., de la Riva, C., Christensen, J., Ostergaard, K., and Emson, P.C. (1996). NMDA and kainate-evoked release of nitric oxide and classical transmitters in the rat striatum: in vivo evidence that nitric oxide may play a neuroprotective role. Eur. J. Neurosci. *8*, 2619–2634.

Kosillo, P., Zhang, Y.F., Threlfell, S., and Cragg, S.J. (2016). Cortical Control of Striatal Dopamine Transmission via Striatal Cholinergic Interneurons. Cereb. Cortex. Published online August 27, 2016. https://doi.org/10.1093/cercor/bhw252.

Kreitzer, A.C., and Malenka, R.C. (2005). Dopamine modulation of state-dependent endocannabinoid release and long-term depression in the striatum. J. Neurosci. *25*, 10537–10545.

otoxin-MII-sensitive presynaptic nicotinic acetylcholine receptors in rat striatum. J. Pharmacol. Exp. Ther. *302*, 197–204.

Morales, M., and Wang, S.D. (2002). Differential composition of 5-hydroxytryptamine3 receptors synthesized in the rat CNS and peripheral nervous system. J. Neurosci. *22*, 6732–6741.

Narushima, M., Uchigashima, M., Hashimoto, K., Watanabe, M., and Kano, M. (2006). Depolarization-induced suppression of inhibition mediated by endocannabinoids at synapses from fast-spiking interneurons to medium spiny neurons in the striatum. Eur. J. Neurosci. *24*, 2246–2252.

Narushima, M., Uchigashima, M., Fukaya, M., Matsui, M., Manabe, T., Hashimoto, K., Watanabe, M., and Kano, M. (2007). Tonic enhancement of endocannabinoid-mediated retrograde suppression of inhibition by cholinergic interneuron activity in the striatum. J. Neurosci. *27*, 496–506.

Nowend, K.L., Arizzi, M., Carlson, B.B., and Salamone, J.D. (2001). D1 or D2 antagonism in nucleus accumbens core or dorsomedial shell suppresses lever pressing for food but leads to compensatory increases in chow consumption. Pharmacol. Biochem. Behav. *69*, 373–382.

Ogasawara, D., Deng, H., Viader, A., Baggelaar, M.P., Breman, A., den Dulk, H., van den Nieuwendijk, A.M., Soethoudt, M., van der Wel, T., Zhou, J., et al. (2016). Rapid and profound rewiring of brain lipid signaling networks by acute diacylglycerol lipase inhibition. Proc. Natl. Acad. Sci. USA *113*, 26–33.

Oleson, E.B., Beckert, M.V., Morra, J.T., Lansink, C.S., Cachope, R., Abdullah, R.A., Loriaux, A.L., Schetters, D., Pattij, T., Roitman, M.F., et al. (2012). Endocannabinoids shape accumbal encoding of cue-motivated behavior via CB1 receptor activation in the ventral tegmentum. Neuron *73*, 360–373.

Peters, J.M., Harris, J.R., and Kleinschmidt, J.A. (1991). Ultrastructure of the approximately 26S complex containing the approximately 20S cylinder particle (multicatalytic proteinase/proteasome). Eur. J. Cell Biol. *56*, 422–432.

Petreanu, L., Huber, D., Sobczyk, A., and Svoboda, K. (2007). Channelrhodopsin-2-assisted circuit mapping of long-range callosal projections. Nat. Neurosci. *10*, 663–668.

Riegel, A.C., and Lupica, C.R. (2004). Independent presynaptic and postsynaptic mechanisms regulate endocannabinoid signaling at multiple synapses in the ventral tegmental area. J. Neurosci. *24*, 11070–11078.

Robbe, D., Bockaert, J., and Manzoni, O.J. (2002a). Metabotropic glutamate receptor 2/3-dependent long-term depression in the nucleus accumbens is blocked in morphine withdrawn mice. Eur. J. Neurosci. *16*, 2231–2235.

Robbe, D., Kopf, M., Remaury, A., Bockaert, J., and Manzoni, O.J. (2002b). Endogenous cannabinoids mediate long-term synaptic depression in the nucleus accumbens. Proc. Natl. Acad. Sci. USA *99*, 8384–8388.

Ronesi, J., Gerdeman, G.L., and Lovinger, D.M. (2004). Disruption of endocannabinoid release and striatal long-term depression by postsynaptic blockade of endocannabinoid membrane transport. J. Neurosci. *24*, 1673–1679.

Long, J.Z., Li, W., Booker, L., Burston, J.J., Kinsey, S.G., Schlosburg, J.E., Pavón, F.J., Serrano, A.M., Selley, D.E., Parsons, L.H., et al. (2009). Selective blockade of 2-arachidonoylglycerol hydrolysis produces cannabinoid behavioral effects. Nat. Chem. Biol. *5*, 37–44.

Lupica, C.R., Riegel, A.C., and Hoffman, A.F. (2004). Marijuana and cannabinoid regulation of brain reward circuits. Br. J. Pharmacol. *143*, 227–234.

Mathur, B.N., and Lovinger, D.M. (2012). Endocannabinoid-dopamine interactions in striatal synaptic plasticity. Front. Pharmacol. *3*, 66.

Mato, S., Robbe, D., Puente, N., Grandes, P., and Manzoni, O.J. (2005). Presynaptic homeostatic plasticity rescues long-term depression after chronic Delta 9-tetrahydrocannabinol exposure. J. Neurosci. *25*, 11619–11627.

Mato, S., Lafourcade, M., Robbe, D., Bakiri, Y., and Manzoni, O.J. (2008). Role of the cyclic-AMP/PKA cascade and of P/Q-type Ca++ channels in endocannabinoid-mediated long-term depression in the nucleus accumbens. Neuropharmacology *54*, 87–94.

Mogg, A.J., Whiteaker, P., McIntosh, J.M., Marks, M., Collins, A.C., and Wonnacott, S. (2002). Methyllycaconitine is a potent antagonist of alpha-conSesack, S.R., and Grace, A.A. (2010). Cortico-Basal Ganglia reward network: microcircuitry. Neuropsychopharmacology *35*, 27–47.

Sidló, Z., Reggio, P.H., and Rice, M.E. (2008). Inhibition of striatal dopamine release by CB1 receptor activation requires nonsynaptic communication involving GABA, H2O2, and KATP channels. Neurochem. Int. *52*, 80–88.

Smolders, I., Sarre, S., Vanhaesendonck, C., Ebinger, G., and Michotte, Y. (1996). Extracellular striatal dopamine and glutamate after decortication and kainate receptor stimulation, as measured by microdialysis. J. Neurochem. *66*, 2373–2380.

Szabo, B., Muller, T., and Koch, H. (1999). Effects of cannabinoids on dopamine release in the corpus striatum and the nucleus accumbens in vitro. J. Neurochem. *73*, 1084–1089.

Tanimura, A., Yamazaki, M., Hashimotodani, Y., Uchigashima, M., Kawata, S., Abe, M., Kita, Y., Hashimoto, K., Shimizu, T., Watanabe, M., et al. (2010). The endocannabinoid 2-arachidonoylglycerol produced by diacylglycerol lipase alpha mediates retrograde suppression of synaptic transmission. Neuron *65*, 320–327.

Threlfell, S., Lalic, T., Platt, N.J., Jennings, K.A., Deisseroth, K., and Cragg, S.J. (2012). Striatal dopamine release is triggered by synchronized activity in cholinergic interneurons. Neuron *75*, 58–64.

Tzavara, E.T., Wade, M.R., Davis, R.J., El Khoury, M.A., and Nomikos, G.G. (2008). Role of metabotropic glutamate receptor 5 in the procholinergic effects of neuropsychotherapeutic compounds. Synapse *62*, 940–943.

Uchigashima, M., Narushima, M., Fukaya, M., Katona, I., Kano, M., and Watanabe, M. (2007). Subcellular arrangement of molecules for 2-arachidonoyl-glycerol-mediated retrograde signaling and its physiological contribution to synaptic modulation in the striatum. J. Neurosci. *27*, 3663–3676.

Wallmichrath, I., and Szabo, B. (2002). Cannabinoids inhibit striatonigral GABAergic neurotransmission in the mouse. Neuroscience *113*, 671–682.

Wang, H.L., and Morales, M. (2008). Corticotropin-releasing factor binding protein within the ventral tegmental area is expressed in a subset of dopaminergic neurons. J. Comp. Neurol. *509*, 302–318.

Yorgason, J.T., España, R.A., and Jones, S.R. (2011). Demon voltammetry and analysis software: analysis of cocaine-induced alterations in dopamine signaling using multiple kinetic measures. J. Neurosci. Methods *202*, 158–164.

Yun, I.A., Nicola, S.M., and Fields, H.L. (2004). Contrasting effects of dopamine and glutamate receptor antagonist injection in the nucleus accumbens suggest a neural mechanism underlying cue-evoked goal-directed behavior. Eur. J. Neurosci. *20*, 249–263.

Zhang, L., and Warren, R.A. (2002). Muscarinic and nicotinic presynaptic modulation of EPSCs in the nucleus accumbens during postnatal development. J. Neurophysiol. *88*, 3315–3330.

Zhang, S., Qi, J., Li, X., Wang, H.L., Britt, J.P., Hoffman, A.F., Bonci, A., Lupica, C.R., and Morales, M. (2015). Dopaminergic and glutamatergic microdomains in a subset of rodent mesoaccumbens axons. Nat. Neurosci. *18*, 386–392.

Zhou, F.M., Liang, Y., and Dani, J.A. (2001). Endogenous nicotinic cholinergic activity regulates dopamine release in the striatum. Nat. Neurosci. *4*, 1224–1229.

CellPress

STAR METHODS

KEY RESOURCES TABLE

REAGENT or RESOURCE	SOURCE	IDENTIFIER
Antibodies		
Goat polyclonal anti-ChAT	EMD Millipore	Cat# ab144P, RRID: AB_2079751
Mouse monoclonal anti-TH	EMD Millipore	Cat# MAB318, RRID: AB_2201528
Rabbit polyclonal anti-GluR1	Frontier Institute	Cat# GluA1-Rb-Af690, RRID: AB_2571752
Rabbit polyclonal anti-GluR2	Frontier Institute	Cat# GluR2C-Rb-Af1050, RRID: AB_2201528
Rabbit polyclonal anti-CB1	Frontier Institute	Cat# CB1-Rb-Af380, RRID: AB_2571591
Guinea pig polyclonal anti-VGluT1	Frontier Institute	Cat# VGluT1-GP-Af570, RRID: AB_2571618
Alexa Fluor-488-rabbit	Jackson Immunoresearch	Cat#711-545-152, RRID: AB_2313584
Alexa Fluor-594-mouse	Jackson Immunoresearch	Cat# 715-585-150, RRID: AB_2340854
Anti-rabbit-Ig coupled to 1.4-nm gold	Nanoprobes	Cat# 2003
Bacterial and Virus Strains		
AAV1.CamKIIa.hChR2(H134R)-eYFP.WPRE.hGH	Penn Vector Core	Addgene26969P
rAAV hybrid serotype 1/2 rAAV plasmid CamkP-EGFP	Universidad Complutense, Madrid	Virus 8 Guzman lab
rAAV hybrid serotype 1/2 rAAV plasmid CamkP-CRE	Universidad Complutense, Madrid	Virus 9 Guzman lab
AAV5.EF1.DIO.hChR2(H134R)-eYFP.WPRE.hGH	Penn Vector Core	Addgene20298P
Chemicals, Peptides, and Recombinant Proteins		
PNU 120596	Tocris Bioscience	Cat#2498; CAS: 501925-31-1
PNU 282987	Tocris Bioscience	Cat#2303; CAS: 123464-89-1
Picrotoxin	Sigma-Aldrich	P1675; CAS: 124-87-8
[35S]- and [33P]-labeled single-stranded antisense or sense of CB1 receptor probes	NIDA	N/A
R(+)-SCH-23390 hydrochloride	Sigma-Aldrich	125941-87-9
Mecamylamine	Sigma-Aldrich	826-39-1
JZL-184	Cayman	13158
AM-251	Cayman	71670
WIN55-212-2	Sigma-Aldrich	W102-25MG
URB597	Cayman	CAS 546141-08-6

Methyllycaconitine	Sigma-Aldrich	112825-05-5
DO34	Laboratory of Dr. Benjamin Cravatt	N/A
WIN 55,212-2	Tocris	131543-23-2
Experimental Models: Organisms/Strains		
Mouse: C57BL/6J	Jackson Laboratories	Cat#000664; RRID: IMSR_JAX:000664
Mouse: Ai14: Gt(ROSA)26Sortm14(CAG-tdTomato)Hze	Jackson Laboratories	Cat#007914; RRID: IMSR_JAX:007914
Mouse: CB1$^{flox/flox}$	NIAAA	N/A
Mouse: Chat::cre	Jackson Laboratories	Cat#006410; RRID: IMSR_JAX:006410
Software and Algorithms		
Mini Analysis	Synaptosoft	N/A
Clampex/Clampfit 10.3	Molecular Devices	N/A
Demon EChem Software	Custom	N/A

CONTACT FOR REAGENTS AND RESOURCE SHARING

Further information and requests for reagents and resources should be directed to, and will be fulfilled by the Lead Contact, Dr. David Lovinger (lovindav@mail.nih.gov).

EXPERIMENTAL MODEL AND SUBJECT DETAILS

Animals

Group housed (4 per cage) in a 12 hr cycle adult male ChAT-IRES-Cre mice, B6;129S6-Chattm1(cre)Lowl/J (Jackson Laboratory, ME), weighing an average of 27 g were used unless otherwise stated. Animals were housed in a temperature-controlled vivarium (24 C) and fed regular laboratory chow with *ad libitum* access to water. These animals were also used to generate a selective knockout of the CB1 receptor (CB1R) from cholinergic neurons. First, CB1$^{flox/flox}$ were obtained from the Fisher's Lane Animal Center maintained by the NIAAA-NIH. CB1$^{flox/flox}$ mice have the endogenous Cnr1 gene, which encodes for the CB1 receptor protein, replaced with a version that has exon 2 flanked on both sides by one pair of loxP sites. Next, homozygous ChAT::Cre mice were mated with C57BL/6J mice to generate heterozygous ChAT::Cre mice (ChAT^{+}/cre). ChAT^{+}::cre mice were then mated with CB1$^{flox/flox}$, resulting in a 1:1 ratio of ChAT^{+}::cre CB1^{+}/^{flox}: ChAT$^{+/+}$ CB1$^{+/flox}$ pups. The generated ChAT^{+}::creCB1$^{+/flox}$ animals were crossed with CB1$^{flox/flox}$ mice, resulting in a 1:1:1:1 ratio of the following genotypes: ChAT$^{+/+}$CB1$^{+/flox}$; ChAT^{+}::cre/CB1$^{+/flox}$; ChAT$^{+/+/}$CB1$^{flox/flox}$ and ChAT^{+}::Cre/CB1$^{flox/flox}$. This mating scheme was continued, as both required breeder genotypes (ChAT^{+}::Cre/CB1$^{+/flox}$ and CB1$^{flox/flox}$) are produced via this mating scheme. ChAT^{+}::Cre/CB1$^{flox/flox}$ were used as experimental mice. After surgery, mice were single housed in a room under a 12-hr light/dark cycle and food/water continued to be available *ad libitum*.

To enable whole cell patch recordings from CINs, ChAT^{+}::cre mice were crossed with Ai14 mice (Jackson Laboratory), which express the fluorescent reporter TdTomato under the control of Cre recombinase. Male C57BL/6J mice (10-15 weeks old, Jackson Laboratory) were used for experiments in which ChR2 was expressed in mPFC projections and for miniature EPSC (mEPSC) recordings. All experiments and procedures were approved by the University of Maryland School of Medicine's Institutional Animal Care and Use Committee protocols and the NIH Guide for the Care and Use of animals.

METHOD DETAILS

Stereotaxic virus injection

Mice were positioned in a stereotaxic frame under anesthesia with isoflurane (3% induction, 2% maintenance). AAV-EIF1a-DIO-hChR2-EYFP was injected bilaterally (300 nl/side) into the NAc (+ 1.2 anteroposterior, ± 1.2 mediolateral and 3.8 dorsoventral, relative to bregma) using a Hamilton 800 series syringe. For some experiments mice were additionally transfected with a recombinant AAV vector encoding cre (or EGFP as a control) under the control of the CaMKII promoter into the mPFC (+ 1.9 anteroposterior, ± 0.5 mediolateral and 2.5 dorsoventral).

optical stimulation and fast-scan cyclic voltammetry

At least 4-8 weeks after virus injection (AAV-EIF1a-DIO-hChR2-EYFP), ChAT::Cre mice were anaesthetized with urethane (1.5 g/kg i.p.) and placed in an stereotaxic frame. A glass-encased cylindrical carbon fiber (Goodfellow, PA) (7 m diameter, 150-

200 m exposed length) was aimed to the NAc (AP +1.0 mm; L +1.2 mm; V 3.7-4.2 mm). The optical fiber was lowered with a lateral angle of 15 (AP +1.0; L +2.2 mm; V 3.8 mm). DA was evoked with optical stimulation triggered with 20 pulses at 20 Hz trains.

optical stimulation and fast-scan cyclic voltammetry

At least 4-8 weeks after virus injection, mice brain slices were prepared (Cachope et al., 2012). Expression of ChR2-eYFP was always verified by YFP visualization using an epifluorescence microscope (Olympus MVX10) for each slice before recording. A glass-encased cylindrical carbon fiber (Goodfellow, PA) (7 m diameter, 100-130 m exposed length) was placed into the NAc at a location expressing eYFP. For the majority of experiments performed for this study, optical stimulation was delivered by placing an optical fiber (105 m core diameter, 0.22 NA (Thorlabs, NJ) in apposition to the brain slice. Optical stimulations are represented on the figures as blue rectangles, depicting the time of application. When electrical stimulation was applied; stimuli were delivered by a constant current isolated stimulator (A-M Systems, WA) through a bipolar tungsten electrode in contact with the slice. Extracellular DA release was monitored by FSCV by applying a triangular input waveform from 0.4V to +1.2V and back to 0.4V (versus an Ag/AgCl reference electrode immersed in the bath solution) through the carbon fiber electrode. Cyclic voltammograms were acquired at 100 ms intervals. Ten cyclic voltammograms recorded before stimulation were averaged and subtracted from post-stimulus voltammograms to measure changes in DA levels using Demon acquisition and analysis program (Yorgason et al., 2011).

Electrophysiology

Mouse brain slices were transferred to a recording chamber and placed on an elevated nylon mesh platform. Artificial cerebral spinal fluid (aCSF: 124 mM NaCl, 4.5 mM KCl, 2 mM $CaCl_2$, 1 mM $MgCl_2$, 26 mM $NaHCO_3$, 1.2 mM NaH_2PO_4 and 10 mM glucose, raised to 320-330 mOsm with sucrose) was superfused across the slices at a rate of 1–2 mL min^{-1} at 29–32 C. Whole-cell, voltage-clamp

recordings of excitatory postsynaptic currents (EPSCs) from medium spiny neurons (MSNs) or CINs were carried out using a Multiclamp 700A amplifier (Axon Instruments). Slices were visualized on an Olympus BX50W microscope (Olympus Corporation of America) using a 40x/0.80 n.a. water-immersion objective for localizing cells for whole-cell recordings. Recording pipettes of 2.0–4.0 M were filled with a CsMeSO3-based solution of 300–315 mOsm containing 120 mM $CsMeSO_3$, 5 mM NaCl, 10 mM TEA-Cl, 10 mM HEPES, 5 mM lidocaine bromide, 1.1 mM EGTA, 0.3 mM Na-GTP and 4 mM Mg-ATP. Picrotoxin (50 M) was added to the aCSF for recordings to isolate excitatory transmission. For mEPSC recordings, tetrodotoxin (TTX, 0.5 M) was also included in the aCSF. MSNs were identified based on their capacitance and membrane resistance. CINs were identified by online visualization of cre-dependent TdTomato expression. Cells were held at 60 mV throughout the course of the experiments. Optically evoked EPSCs (oEPSCs) in MSNs or CINs were elicited in brain slices using 470-nm blue light (5-ms exposure time) delivered via field illumination using a High-Power LED Source (LED4D067, Thor Labs). Light intensity was adjusted to produce a maximal oEPSC amplitude of 400 pA (< 100 mW). oEPSCs were evoked once per minute. Asynchronous EPSC (aEPSC) events were recorded in aCSF in which Ca^{2+} was replaced with 4 mM Sr2+, and were analyzed between 50 and 450 ms following the onset of the light pulse. For mEPSC and aEPSC experiments, baselines were recorded for five minutes, followed by sequential five-minute drug applications. Baseline frequencies and amplitudes were averaged over the full 5-minute period, and drug effects were measured for minutes 3 and 4 of each drug application.

hybridization and ChAT immunolabeling

Three ChAT::cre mice were anesthetized with chloral hydrate (35 mg/100 g) and perfused transcardially with 4% (W/V) paraformaldehyde (PF) in 0.1 M phosphate buffer (PB), pH 7.3. Brains were left in 4% PF for 2 hr at 4 C, rinsed with PB and transferred sequentially to 12%, 14% and 18% sucrose solutions in PB. Coronal serial sections of 20 m in thickness were prepared.

in situ

Coronal free-floating sections were processed as described previously (Morales and Wang 2002; Wang and Morales 2008). Sections were hybridized for 16 hr at 55 C in hybridization buffer containing [35S]- and [33P]-labeled single-stranded antisense or sense of rat CB1 receptor probes at 20 107 cpm/ml. Sections were treated with 4 g/ml RNase A at 37 C for 1 hr, washed with 1 x SSC, 50% formamide at 55 C for 1 hr, and with 0.1 x SSC at 68 C for 1 hr. After the last SSC wash, sections were rinsed with PB and incubated for 1 hr in PB supplemented with 4% bovine serum albumin and 0.3% Triton X-100. This was followed by the overnight incubation at 4 C with an anti-ChAT goat antibody (1:50). After rinsing 3 10 min in PB, sections were processed with an ABC kit (Vector Laboratories, Burlingame, CA). The material was incubated for 1 hr at room temperature in a 1:200 dilution of the biotinylated secondary antibody, rinsed with PB, and incubated with avidin-biotinylated horseradish peroxidase for 1 hr. Sections were rinsed and the peroxidase reaction was then developed with 0.05% 3, 3 diaminobenzidine-4 HCl (DAB) and 0.03% hydrogen peroxide (H2O2). Free-floating sections were mounted on coated slides. Slides were exposed in the dark at 4C for four weeks prior to development.

Fluorescence microscopy and image analysis for immunodetection of AMPA receptors on DA terminals

Fixed mouse coronal brain sections (40 m) were incubated for 1 hr in PB supplemented with 4% BSA and 0.3% Triton X-100. Sec-

tions were then incubated with cocktails of primary antibodies: rabbit-anti-GluR1 (GluR1C-Rb-Af692-1; Frontier Institute, 1:500 dilution) + mouse-anti-TH (MAB318; EMD Millipore, 1:1000 dilution); or rabbit-anti-GluR2 (GluR2C-Rb-Af286; Frontier Institute, 1:500 dilution) + mouse-anti-TH (MAB318; EMD Millipore, 1:1000 dilution) overnight at 4C. Fluorescent images were collected with Olympus FV1000 Confocal System (Olympus, Center Valley, PA).

Electron microscopy

Vibratome brain sections were rinsed with 0.1 M PB (pH 7.3), incubated with 1% (w/v) sodium borohydride in PB for 30 min to inactivate free aldehyde groups, rinsed in PB, and then incubated with blocking solution [1% (v/v) normal goat serum (NGS), 4% (w/v) BSA in PB supplemented with 0.02% (w/v) saponin] for 30 min. Sections were incubated with primary antibodies rabbit-anti-CB1 (1:200, CB1-Rb-Af380, Frontier Institute) + guinea pig-anti-VGluT1 (1:400, VGluT1-GP-Af570, Frontier Institute). Sections were rinsed and incubated overnight at 4 C in the corresponding secondary antibodies: biotinylated goat-anti-guinea pig (VGluT1 detection) + anti-rabbit-IgG coupled to 1.4-nm gold (2003; 1:100 dilution, CB1 detection). Next, sections were processed with an ABC kit, fixed with 0.5% (v/v) osmium tetroxide, and contrasted in 1% (w/v) uranyl acetate. Sections were dehydrated and flat embedded in Durcupan ACM epoxy resin (EMS). Sections were examined and photographed using a Tecnai G^2 12 transmission electron microscope (Fei). Specificity of primary antibodies has been previous described (Zhang et al., 2015).

Behavioral experiments

Male C57BL/6J mice (n = 7) were transduced with a recombinant AAV vector under the control of the CaMKII alpha promoter (AAV1.CamKII .hChR2(II134R)-eYFP; 500 nl) bilaterally into the mPFC. CB1$^{flox/flox}$ (n = 7) transduced with a recombinant AAV vector expressing Cre recombinase under the control of the CaMKII promoter (AAV1.CamKII .4.Cre.SV40; 300 nl) along with a Cre-dependent ChR2 vector (AAV5.EF1a.DIO.hChR2(H134R)-eYFP.WPRE.hGH; 200 nl) bilaterally into the mPFC as described above. Optical

fibers (105 m core diameter, 0.22 NA; Thorlabs, NJ) were implanted bilaterally into the NAc 5-6 weeks following viral transduction. Stereotaxic coordinates for the mPFC and NAc are relative to bregma as follows: mPFC, +1.9 anterioposterior, ± 0.5 mediolateral, 2.5 dorsoventral; NAc, +1.2 anterioposterior, ± 1.2 mediolateral, 3.8 dorsoventral. Mice were tested for optogenetic intracranial self-stimulation (ICSS) of CamKII -expressing inputs to the NAc 1 week following fiber implants.

For self-stimulation experiments, mice were placed in operant chambers (21.6 chm x 17.8 cm x 14 cm; Med Associates, St Albans, VT) equipped with retractable active and inactive levers. An LED light above the lever indicated the active lever. Active lever presses produced 30, 5 ms light pulses delivered at 30 Hz. Inactive lever presses were recorded but had no programmed consequence. Sessions lasted 30 min. Light was delivered by a diode-pumped solid-state laser (473 nm, 150 mW) coupled to 62.5 m core, 0.22 NA optical fiber (Thor Labs), and was split with a fused optical coupler. Light output was 10 mW per split fiber.

For self-stimulation experiments, mice were treated with vehicle, AM251 (0.75 mg/kg), JZL184 (18 mg/kg), or JZL (18 mg/kg) + AM251 (0.75 mg/kg). Injections were administered intraperitoneally and assigned using a Latin square design with a minimum of 3 days between treatments. Pretreatment times were 30 min for AM251 and vehicle, and 120 min for JZL (Long et al., 2009). Drugs were prepared in a 1:1:18 vehicle consisting of emulphor, ethanol, and saline, respectively. For ICSS and local pharmacology experiments, a 26-gauge guide cannula was coupled to an optical fiber (Jennings et al., 2013) and implanted bilaterally in the NAc. Saline (0.5 l), SCH 23390 (1 g/0.5 l) or mecamylamine (10 g/0.5 l) were infused at a rate of 0.25 l/min. Cannulae were left in place for an additional 2 min to allow drug diffusion. Subjects were placed in the behavioral chamber 10 min later. Drug concentrations were chosen based on studies that have previously demonstrated a lack of non-specific locomotor impairments (Nowend et al., 2001; Yun et al., 2004; Collins et al., 2016).

QUANTIFICATION AND STATISTICAL ANALYSIS

Animals were randomly allocated to experimental or control groups and coded key of all specimens was used when possible to blind investigators performing the experiments until data analysis was completed. The primary end of point for each experiment was prospectively assessed and mice that did not survive until this primary end point were not included data analysis. Appropriate parametric statistics were utilized to test our hypotheses. If the data did not meet the assumptions of the intended parametric test (normality, heterogeneity of variance tests) appropriate non-parametric tests were implemented used. Power analysis assumptions were: power = 0.9; alpha = 0.5; two-tailed and an expected difference 50% greater than the observed standard deviation. Unless otherwise indicated, 2-way ANOVA followed by Bonferroni corrections was performed using Prism (GraphPad Software, CA) for analysis of voltammetry recordings as in Cachope et al. (2012). Measurements of EPSCs were made using pClamp software (Molecular Devices). Graphs and statistical analyses were generated using GraphPad Prism 4.0 software (Hearne Scientific Software). EPSC data are reported as percent of baseline (mean ± SEM). Percent baseline measurements of EPSCs reported in the text are the average of the time window (from 31 to 40 min for 40-min recordings in Figures 5C and 5D, and for 26-30 min for 30-min recordings in Figures 6B and 6C). mEPSC frequency and amplitude were analyzed using Mini Analysis (Synaptosoft). mEPSC data are reported for 2 min windows

during baseline and drug recordings. Two-way repeated-measures ANOVA followed by post hoc Bonferroni tests were performed on mEPSC data. Statistical analyses were performed on these same time windows. N values for all figures represent numbers of recorded cells; only one cell was used from each slice, and at least two animals were used for each experimental group. No statistical methods were used to pre-determine sample sizes, but our sample sizes are similar to those reported previously (Atwood et al., 2014). Comparisons of treatments and controls were performed using Student's t tests and one-way ANOVA with Tukey's multiple comparisons post-test.

Data analysis for immunohistochemistry

Single and double-labeled neurons were observed within each traced region at high power (20X objective lens). Double-labeled material was analyzed under bright field and by using epiluminescence to increase the contrast of silver grains (neither dark-field nor bright field optics allow clear visualization of silver grains when co-localized with high concentration of immunoproducts). A cell was considered to express transcripts encoding CB1 receptor when its soma contained concentric aggregates of silver particles above background levels. A neuron was considered to express ChAT immunoreactivity (IR) when its soma was clearly labeled as brown.

Ultrastructural analysis of brain tissue

Serial ultrathin sections of the nucleus accumbens (bregma 2.76 mm to 0.96 mm) from 4 male ChAT::cre mice. Synaptic contacts were classified according to their morphology and immunolabel, and photographed at a magnification of 6,800–13,000 . The morphological criteria used for identification and classification of cellular components observed in these thin sections were as previously described (Peters et al., 1991). Type I synapses, here referred as asymmetric synapses, were defined by the presence of contiguous synaptic vesicles in the presynaptic AT and a thick postsynaptic density (PSD) greater than 40 nm (Peters et al., 1991). Type II synapses, here referred as symmetric synapses, were defined by the presence of contiguous synaptic vesicles in the presynaptic AT and a thin PSD (Peters et al., 1991). Serial sections were obtained to determine the type of synapse. In the serial

sections, a terminal containing greater than five immunogold particles were considered as an immunopositive terminal. Pictures were adjusted to match contrast and brightness by using Adobe Photoshop (Adobe Systems). This experiment was successfully repeated three times. Electron microscopy and confocal analysis quantification occurred blindly. No statistical methods were used to predetermine sample sizes but our sample sizes are similar to those reported in previous publications (Zhang et al., 2015). Behavioral data used Shapiro-Wilk normality tests and 1 or 2-way ANOVA followed by Scheffe and Bonferroni corrections. Alpha was set at 0.05.